



FACULTY OF MATHEMATICS,
PHYSICS AND INFORMATICS
Comenius University
Bratislava

Local Limit Disorder Characteristics of Superconducting Radio Frequency Cavities II.

arXiv:2409.04203

*Resonant Frequency Shift in the Vicinity of T_c and Quality within the
Dynes Superconductor Theory Approach*

František Herman

Slovak Academic and Scientific Programme

S A S P R O 2



FACULTY OF MATHEMATICS,
PHYSICS AND INFORMATICS
Comenius University
Bratislava

Students/Collaborators



Lucia Gelenekyová



Marcel Polák



Anastasiya Lebedeva



Richard Hlubina

Collaborator

Administrative Support



Rebeka Laučíková



Katarína Matejčíková



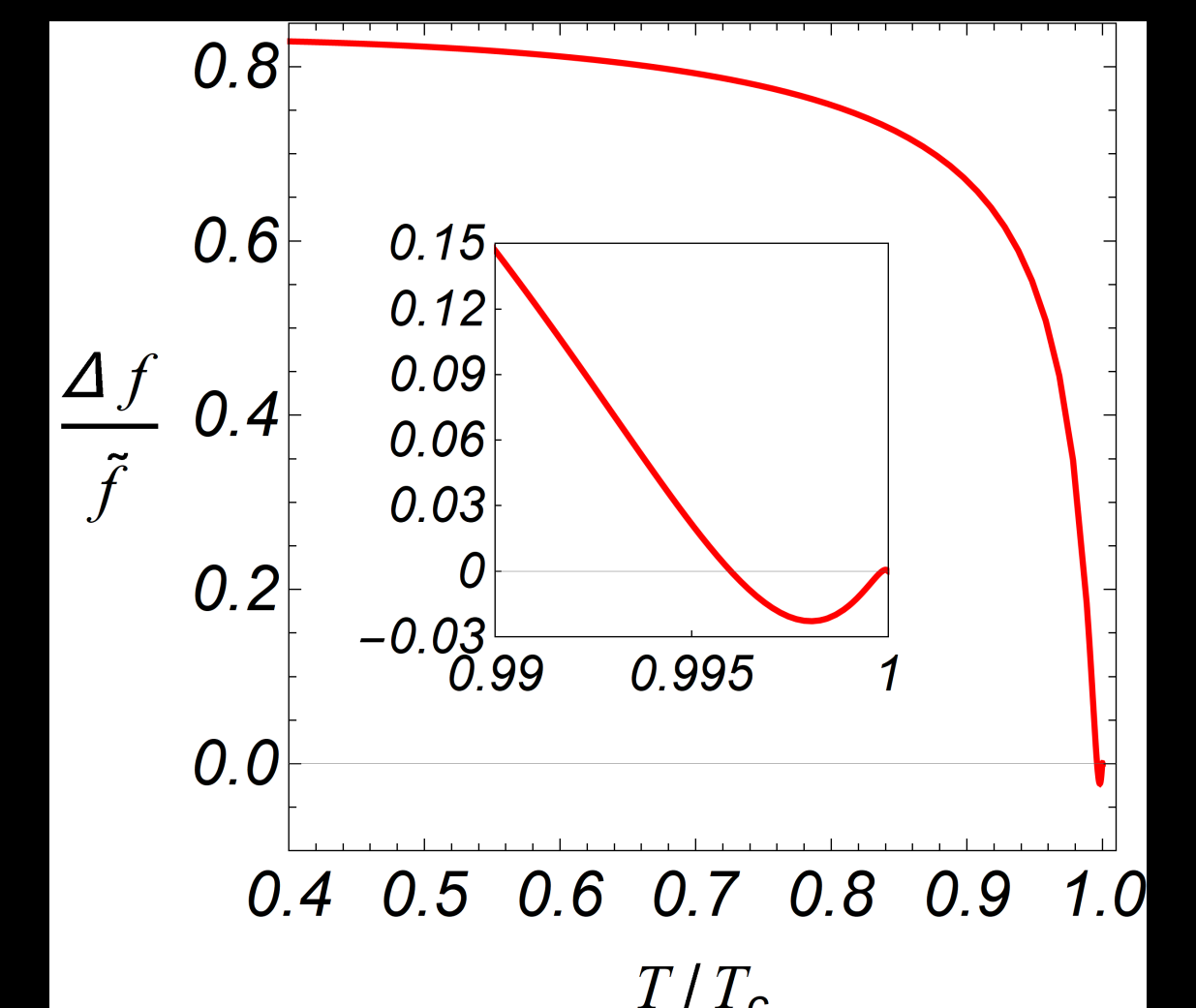
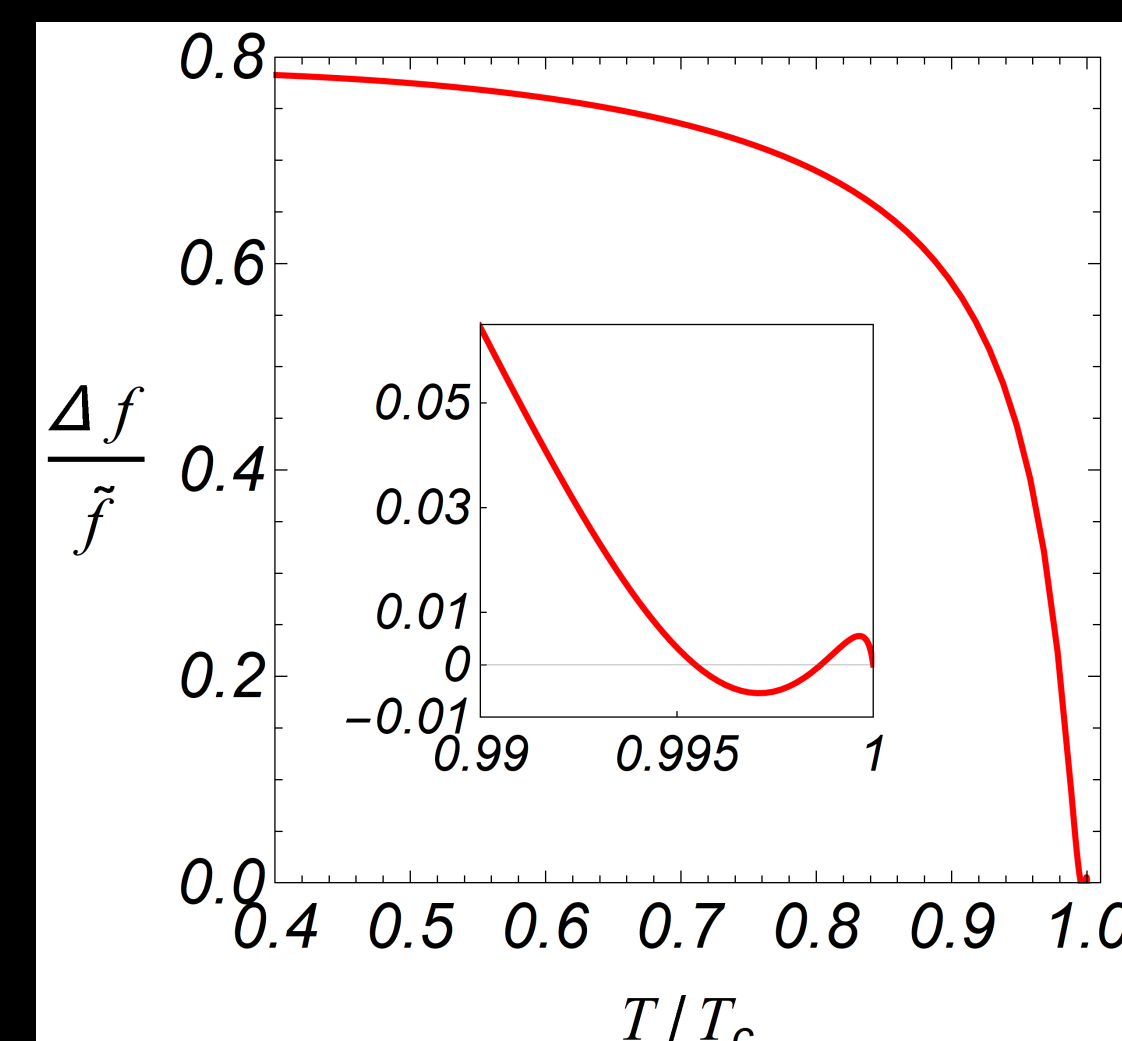
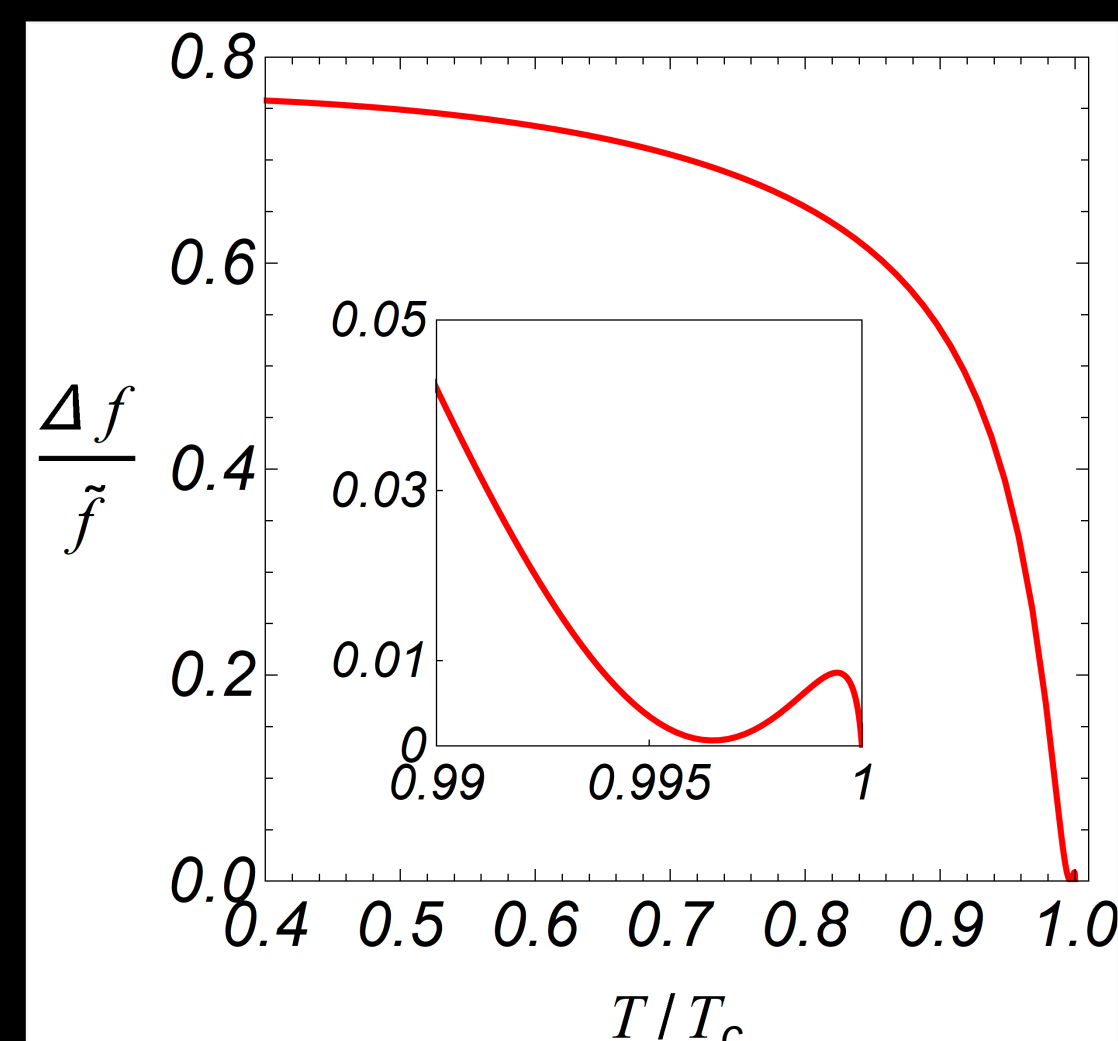
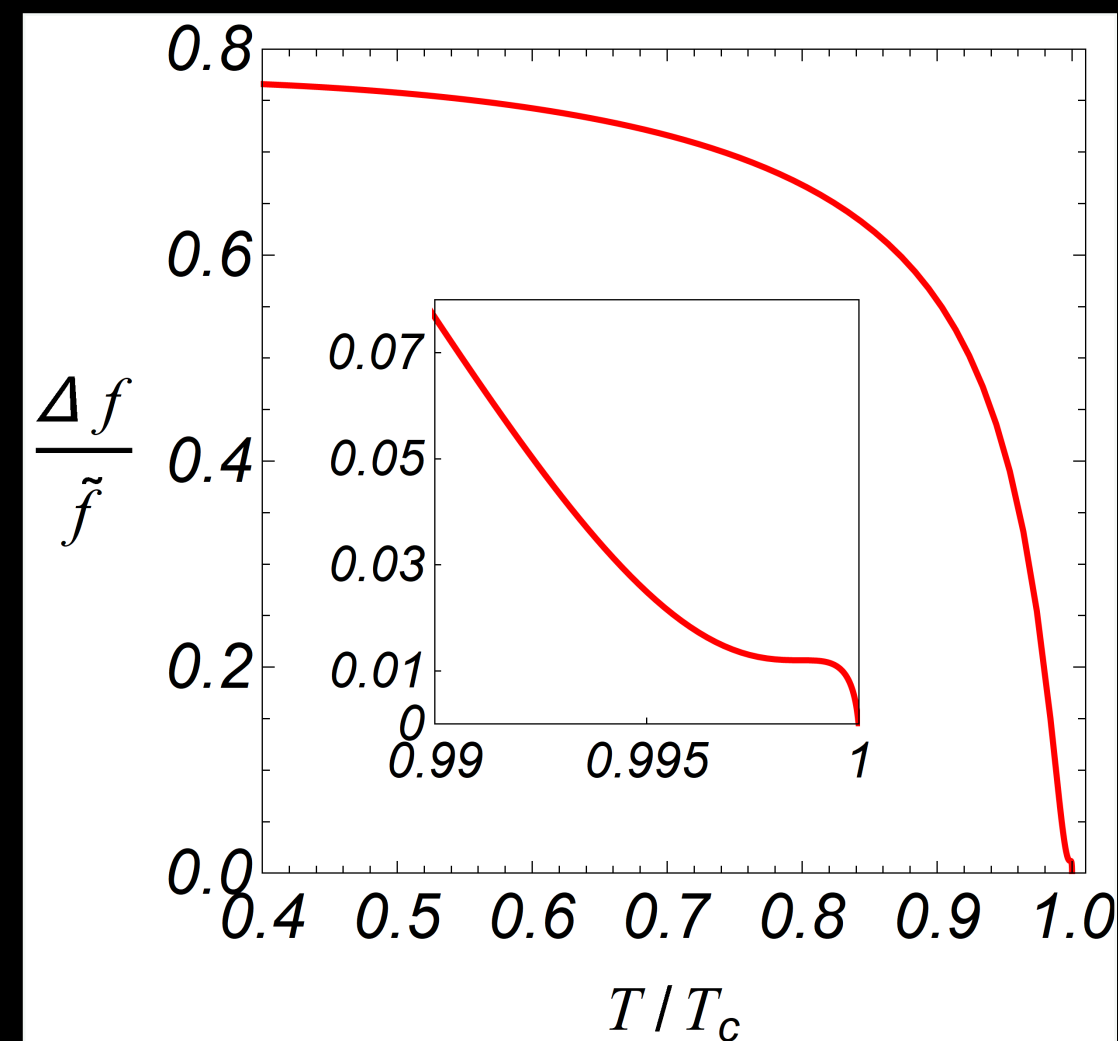
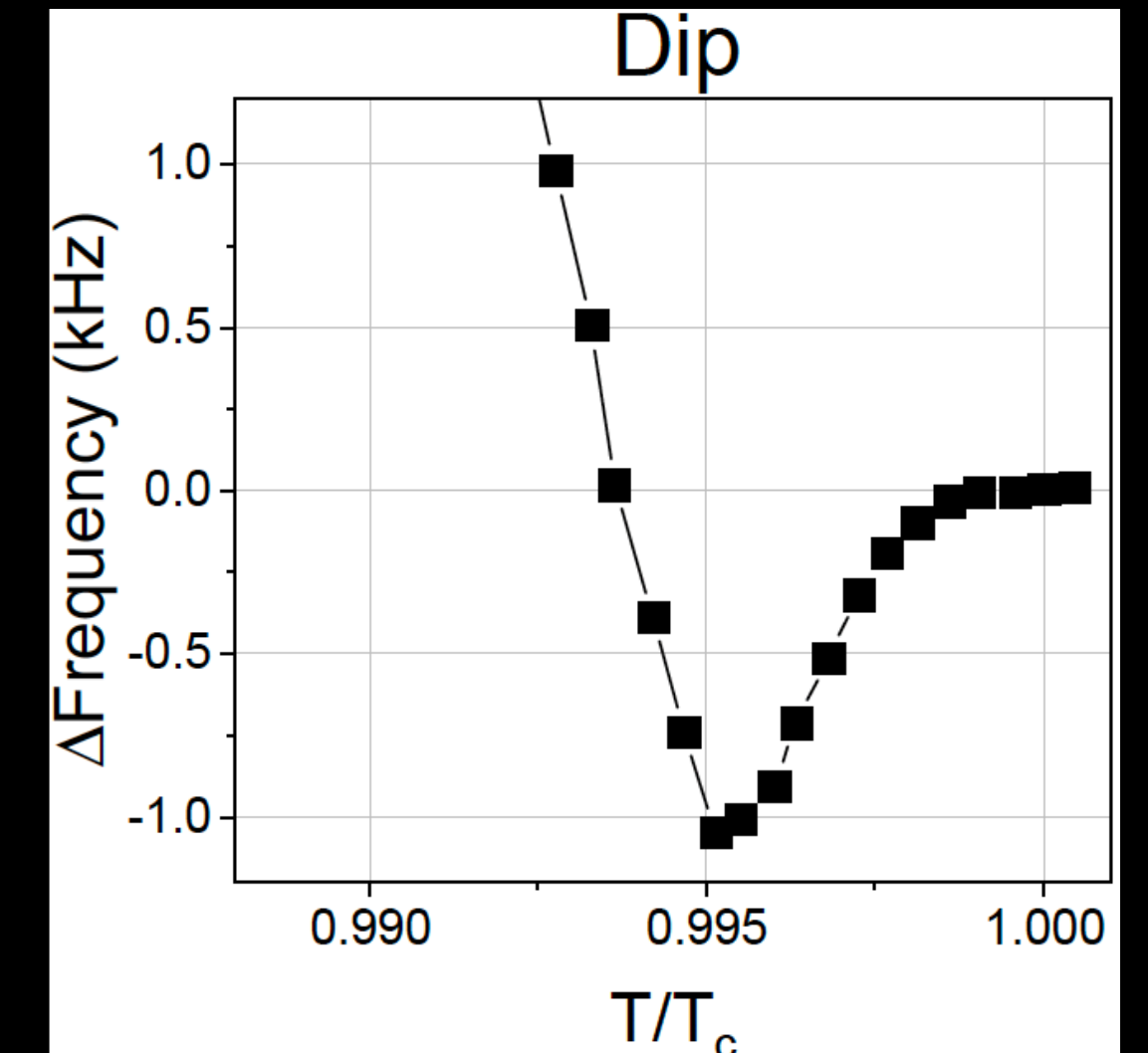
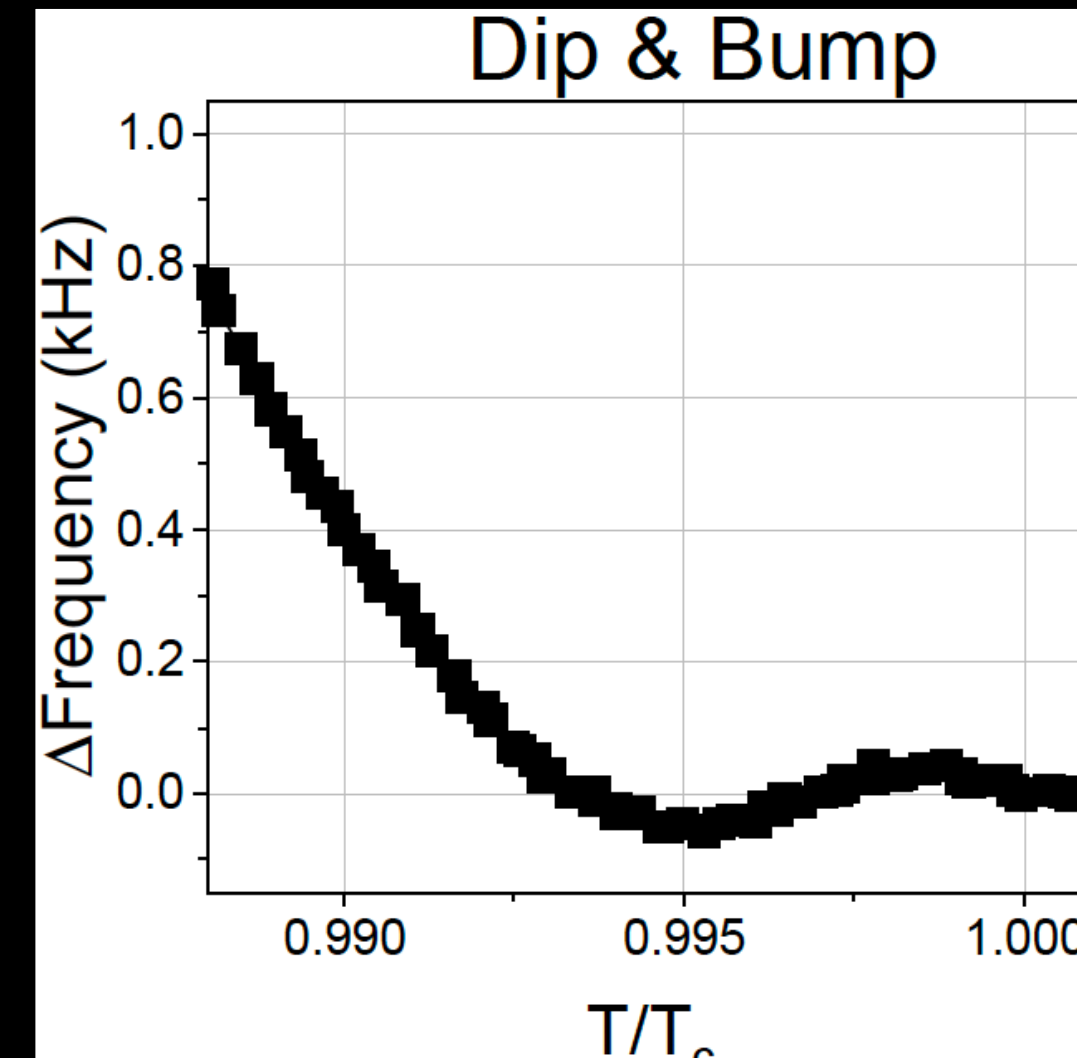
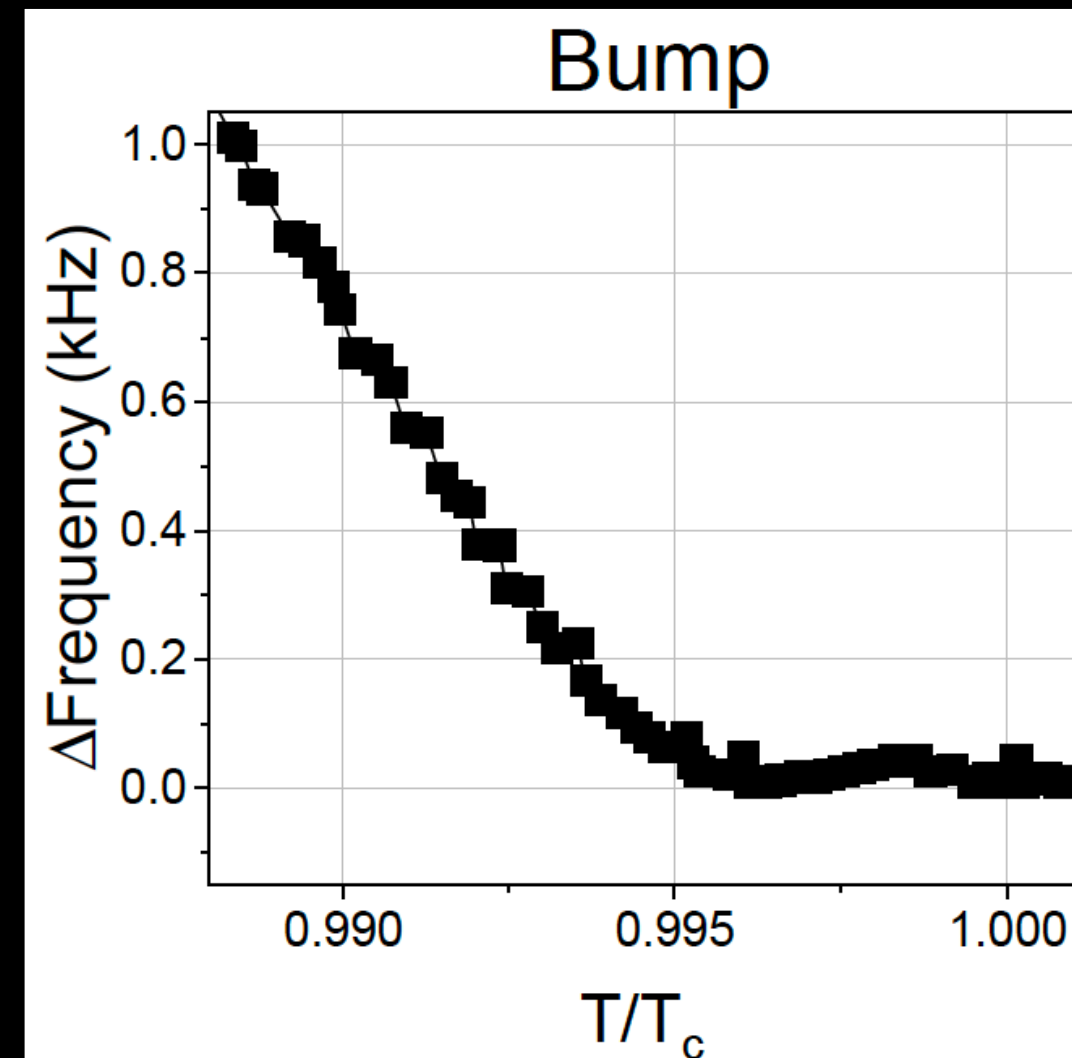
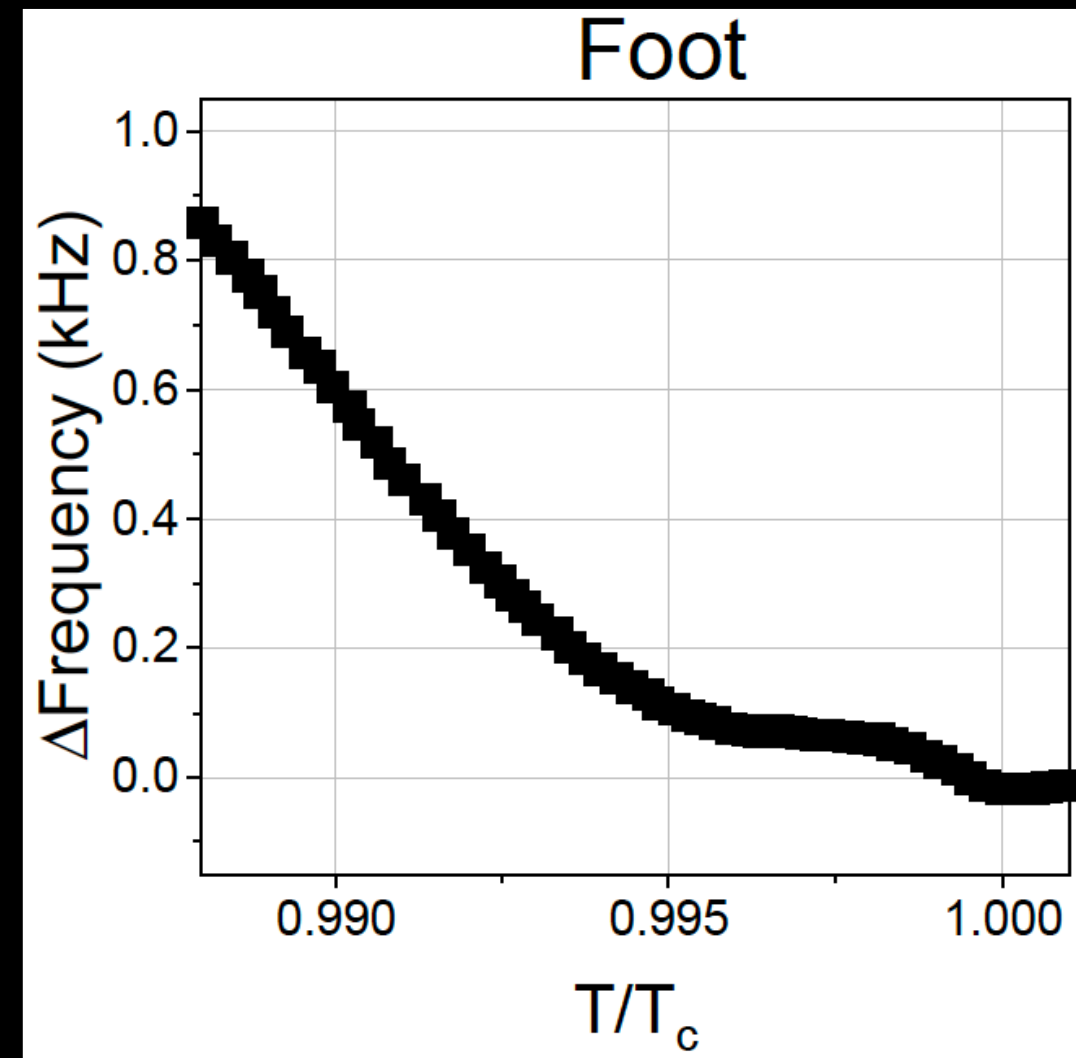
Matúš Hladký

Slovak Academic and Scientific Programme

S A S P R O 2

Motivation: Conclusions from TTCM-Fermilab

D. Bafia et al., arXiv:2103.10601v2



Dynes Superconductor

- Internally consistent extension of the BCS superconductor including (simultaneously present) pair-breaking and pair-conserving scattering processes in general case.
- Capable to describe electromagnetic and thermodynamic response.
- Applicable at low (density of states) and also higher (coherence peak) temperatures.
- Applicable at high disorder (MoC - superconductor-insulator transition) and low disorder (Nb-SRF motivated)
- Mathematical formulation using Green function method:

$$\hat{G}(\mathbf{k}, \omega) = \frac{1}{2} \delta \ln [\epsilon_{\mathbf{k}}^2 - \epsilon(\omega)^2],$$

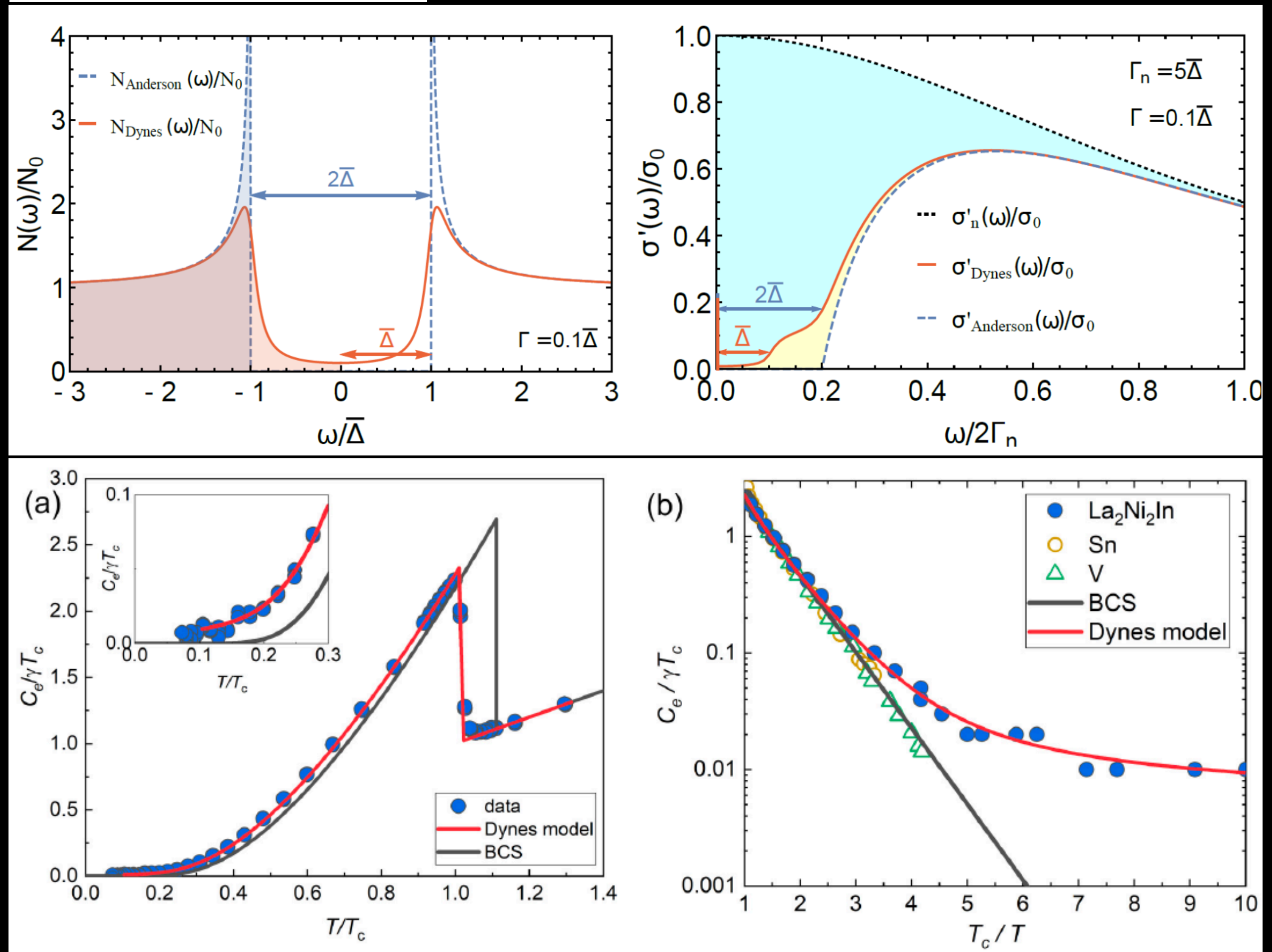
$$\delta = \tau_0 \partial_{\omega} - \tau_1 \partial_{\Delta} - \tau_3 \partial_{\epsilon_{\mathbf{k}}}$$

and temperature = 5 energy scales.

$$\epsilon(\omega) = \sqrt{(\omega + i\Gamma)^2 - \Delta^2 + i\Gamma_s}$$

Electromagnetic properties and optical conductivity

Phys. Rev. B **96**, 014509



Maiwald et al., PRB **102**, 165125 (2020)

Dynes Superconductor

Electromagnetic properties and optical conductivity, formulation

- Green function parametrisation:

$$\Delta(\omega) = \bar{\Delta} / \left(1 + \frac{i\Gamma}{\omega}\right), \quad Z(\omega) = \left(1 + \frac{i\Gamma}{\omega}\right) \left(1 + \frac{i\Gamma_s}{\Omega(\omega)}\right)$$

$$\Omega(\omega) = \sqrt{(\omega + i\Gamma)^2 - \bar{\Delta}^2} \quad \text{and} \quad \bar{\Delta} = \bar{\Delta}(T)$$

- Green function parametrisation:

$$n(\omega) = n_1(\omega) + in_2(\omega) = \frac{\omega}{\sqrt{\omega^2 - \Delta^2(\omega)}} = \frac{\omega + i\Gamma}{\Omega(\omega)}$$

$$p(\omega) = p_1(\omega) + ip_2(\omega) = \frac{\Delta(\omega)}{\sqrt{\omega^2 - \Delta^2(\omega)}} = \frac{\bar{\Delta}}{\Omega(\omega)}$$

$$\begin{aligned} \epsilon(\omega) = \epsilon_1(\omega) + i\epsilon_2(\omega) &= Z(\omega) \sqrt{\omega^2 - \Delta^2(\omega)} \\ &= \Omega(\omega) + i\Gamma_s. \end{aligned}$$

- Resulting formulation

$$\sigma_s(\omega) = \frac{iD_0}{\omega} \int_{-\infty}^{\infty} d\nu \tanh\left(\frac{\nu}{2T}\right) H(\nu + \omega, \nu).$$

$D_0 = ne^2/m$ is the normal-state Drude weight and

$$H_1(x, y) = \frac{1 + n(x)n^*(y) + p(x)p^*(y)}{2[\epsilon^*(y) - \epsilon(x)]},$$

$$H_2(x, y) = \frac{1 - n(x)n(y) - p(x)p(y)}{2[\epsilon(y) + \epsilon(x)]},$$

$$H(x, y) = H_1(x, y) + H_2(x, y)$$

Dynes Superconductor

Implications towards the superconductive cavities: Coherence peak and Imaginary part of DC Conductivity

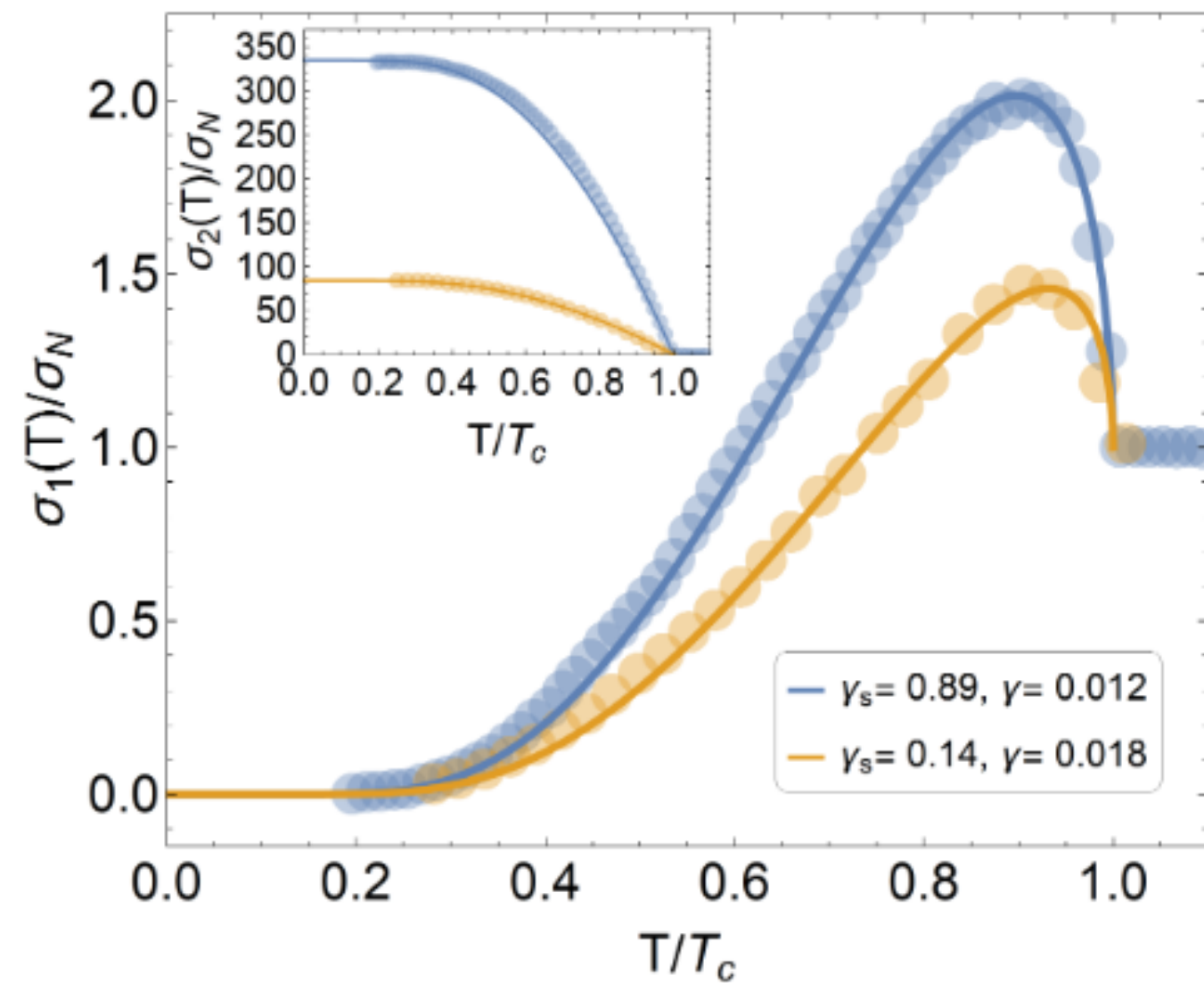


FIG. 9. Real and imaginary parts of the conductivities of the two samples from Fig. 4 in [13] (symbols), together with their fits by the theory of Dynes superconductors with the strong-coupling corrections described for both samples by $x = 1.145$ (lines).

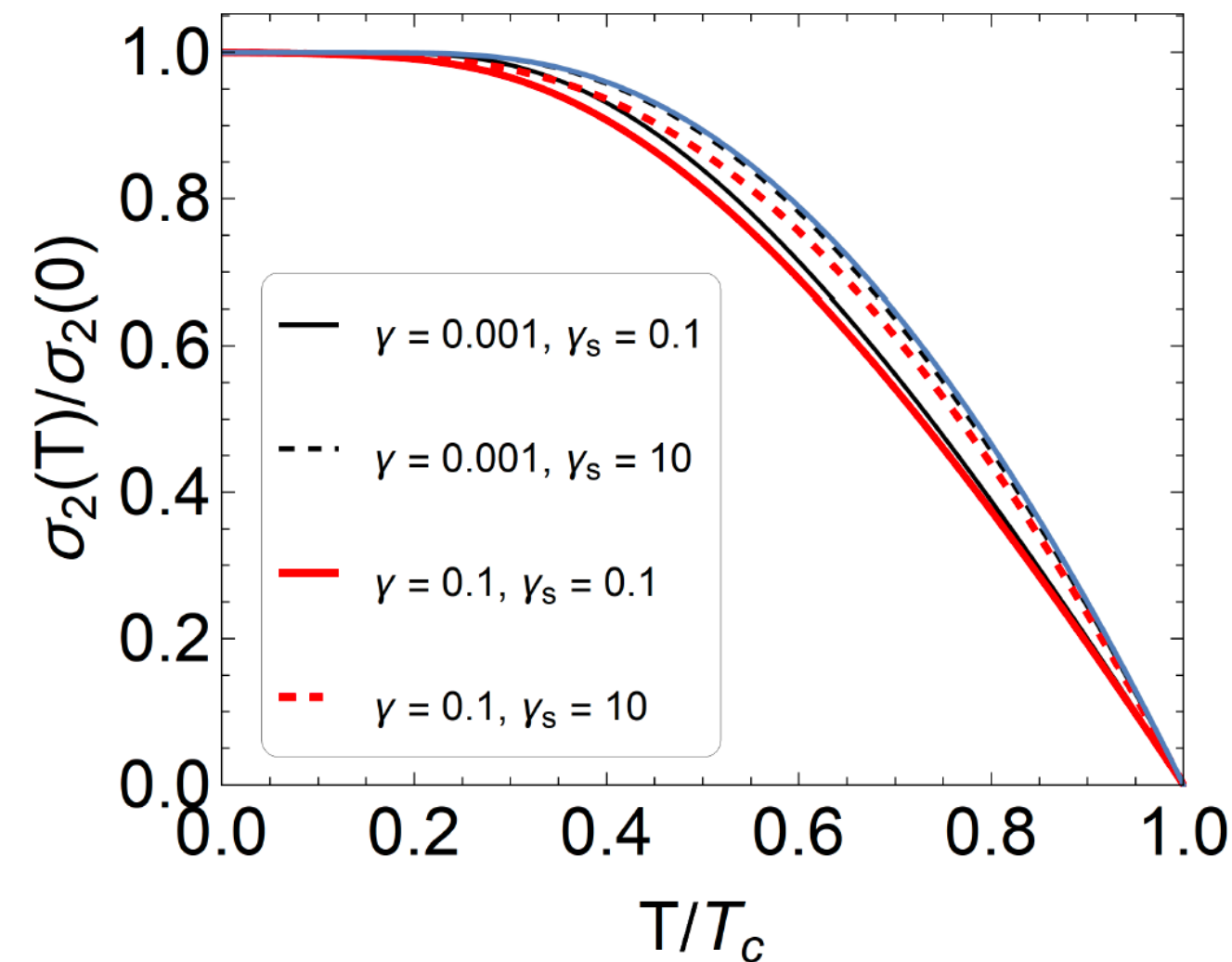


FIG. 6. Temperature dependence of the imaginary part of the microwave conductivity $\sigma_2(T)/\sigma_2(0)$ for several choices of γ and γ_s . Note that when γ_s decreases and γ increases, the curves are pushed slightly downwards with respect to Eq. (14), which is shown by the blue line.

$$\Delta(T) = x\Delta_{\text{BCS}}(T)$$

x - strong coupling correction

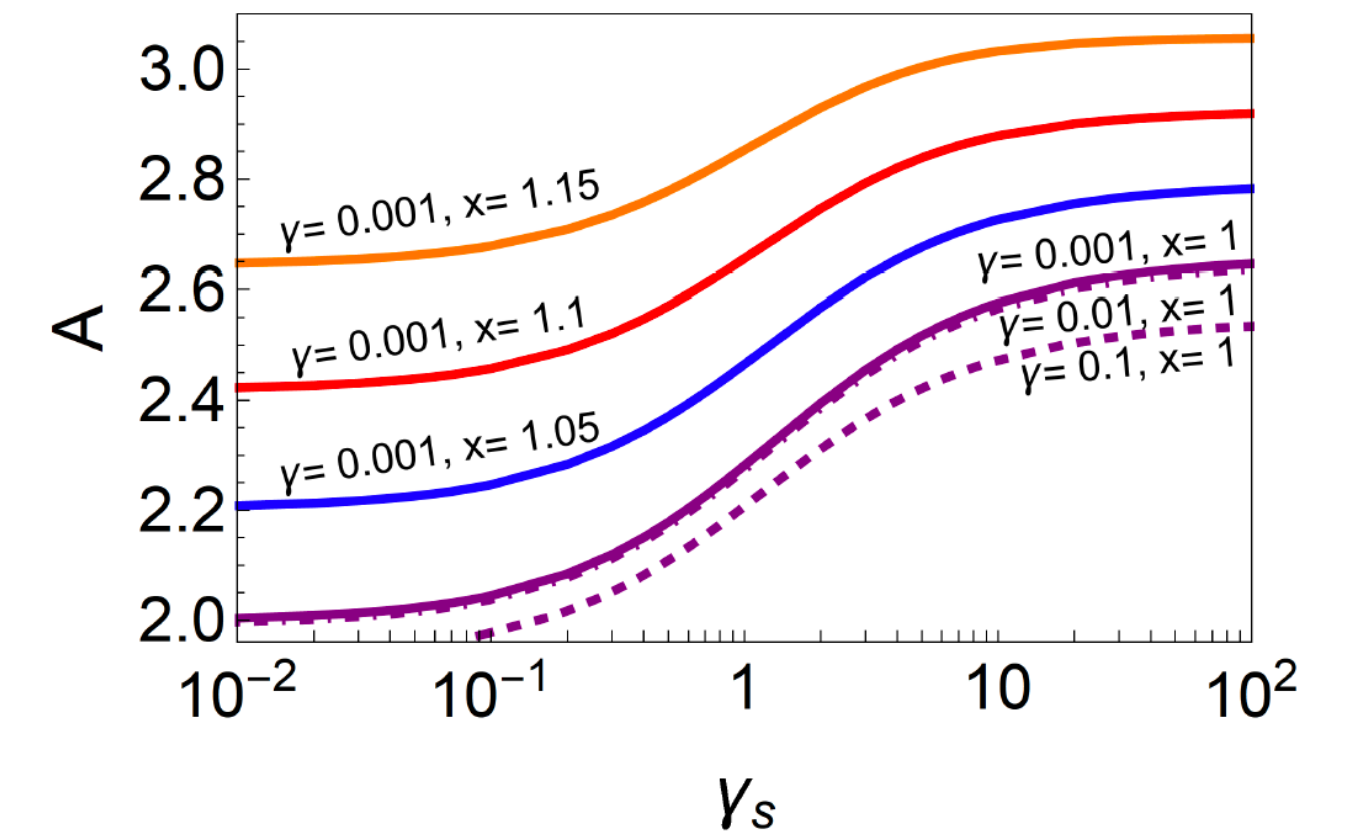


FIG. 7. Coefficient A describing the T -dependence of the imaginary part of the microwave conductivity close to T_c , $\sigma_2(T)/\sigma_2(0) = A(1 - T/T_c)$, plotted as a function of γ_s for several values of γ and x . Note that A depends only very weakly on γ in the limit of small pair breaking.

Surface Impedance (Z) & microwave conductivity (σ)

$$\frac{Z_s}{Z_n} = \frac{R_s + iX_s}{R_n + iX_n} = \left(\frac{\sigma_1 - i\sigma_2}{\sigma_n} \right)^k$$

- R - surface resistance, X - surface reactance

- More convenient form:

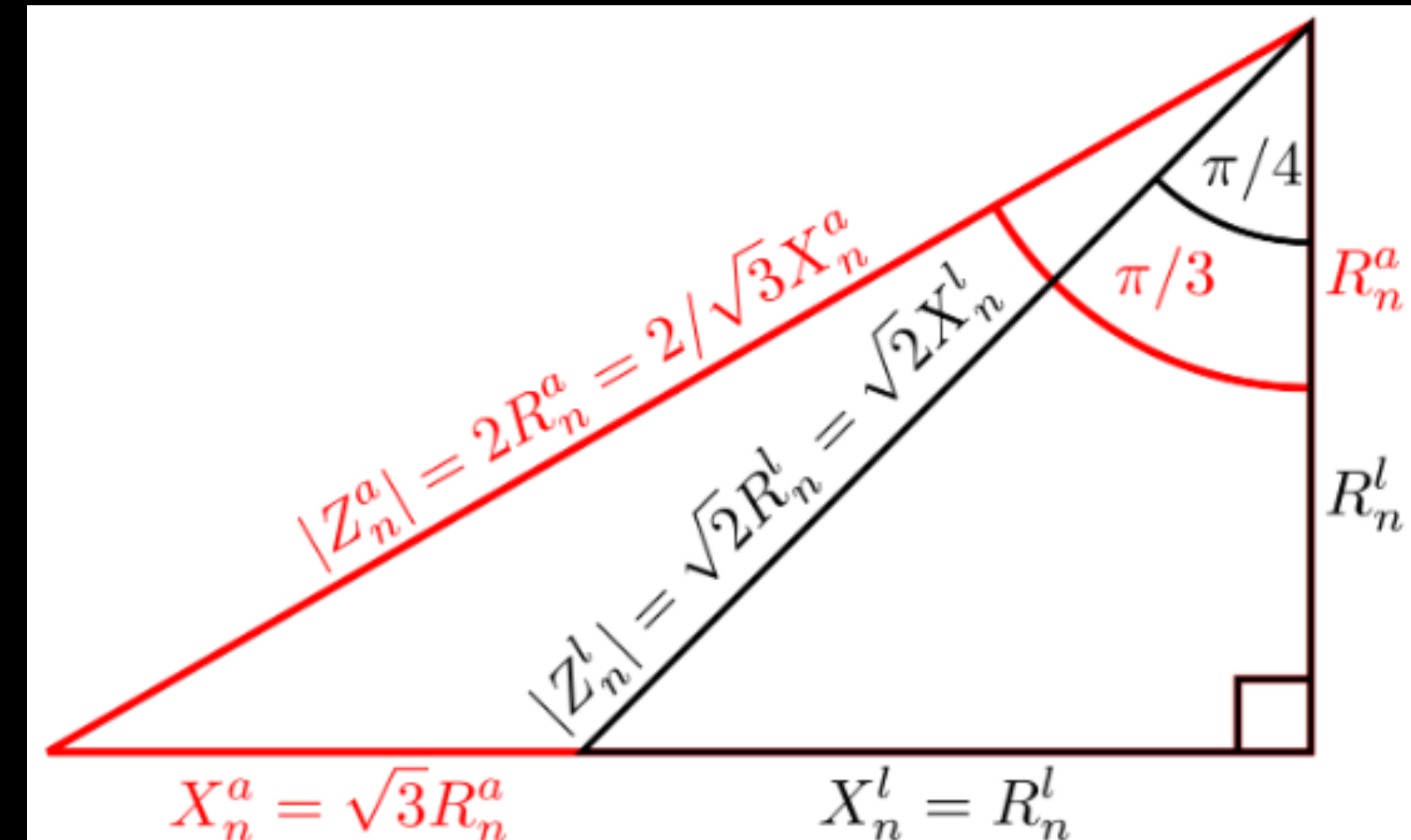
$$Z_s = |Z_n| \left(\frac{|\sigma_s|}{|\sigma_n|} \right)^k e^{i(\alpha_n - k\delta\varphi)}$$

- Simple formulation of superconducting state properties:

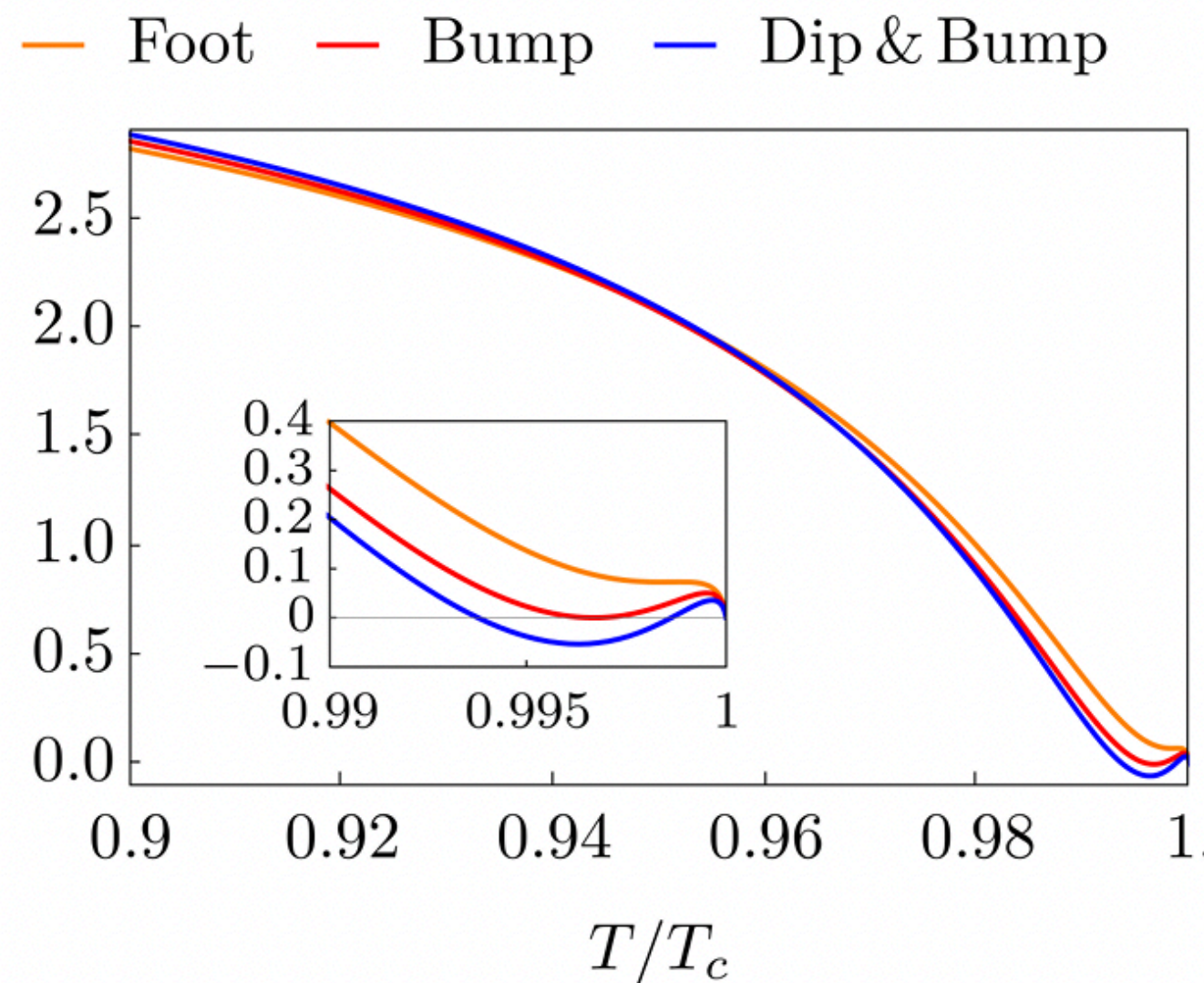
$$R_s = |Z_n| \left(\frac{|\sigma_s|}{|\sigma_n|} \right)^k \cos(\alpha_n - k\delta\varphi)$$

$$X_s = |Z_n| \left(\frac{|\sigma_s|}{|\sigma_n|} \right)^k \sin(\alpha_n - k\delta\varphi)$$

- Normal state parametrization for $\omega\tau \rightarrow 0$.

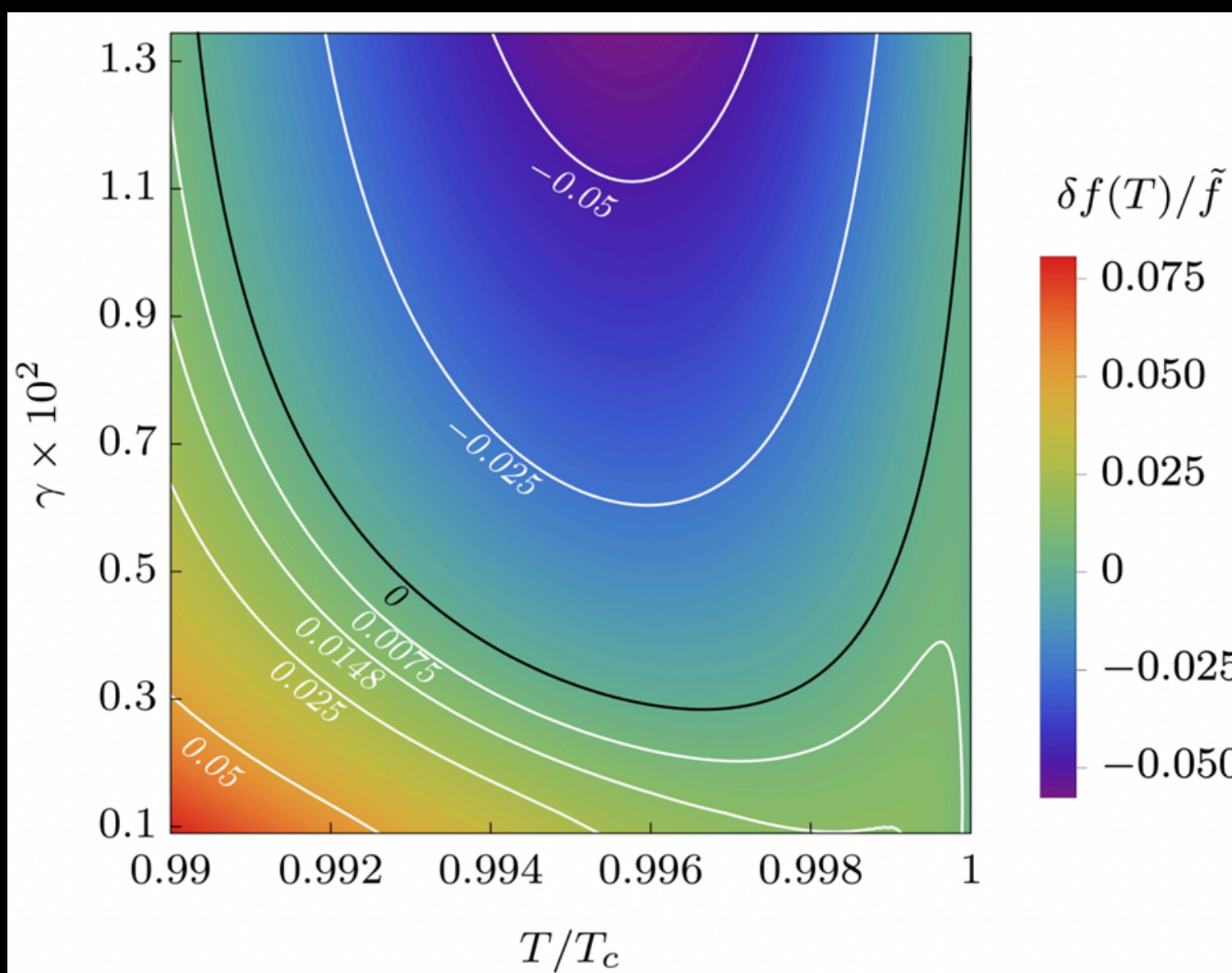
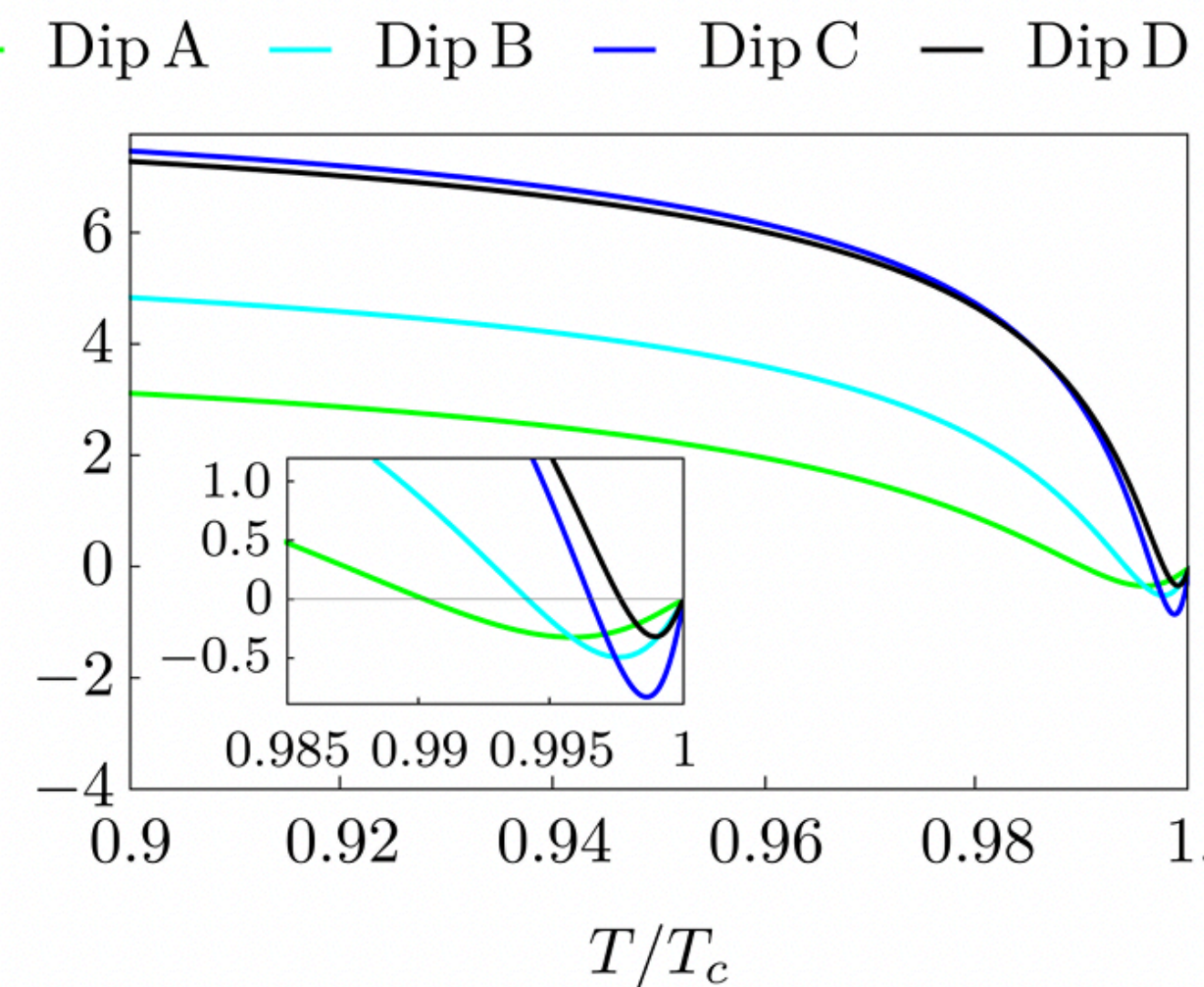


Frequency Shift - different regimes

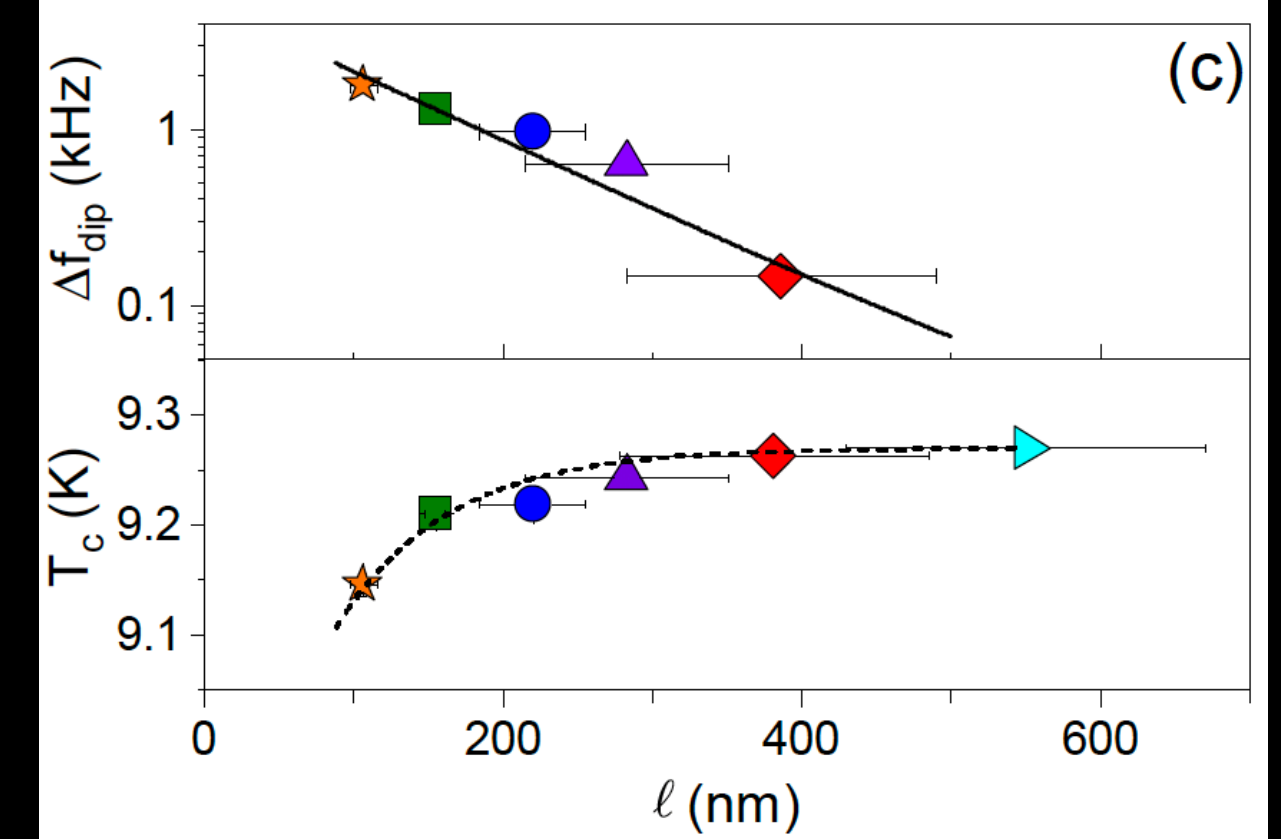
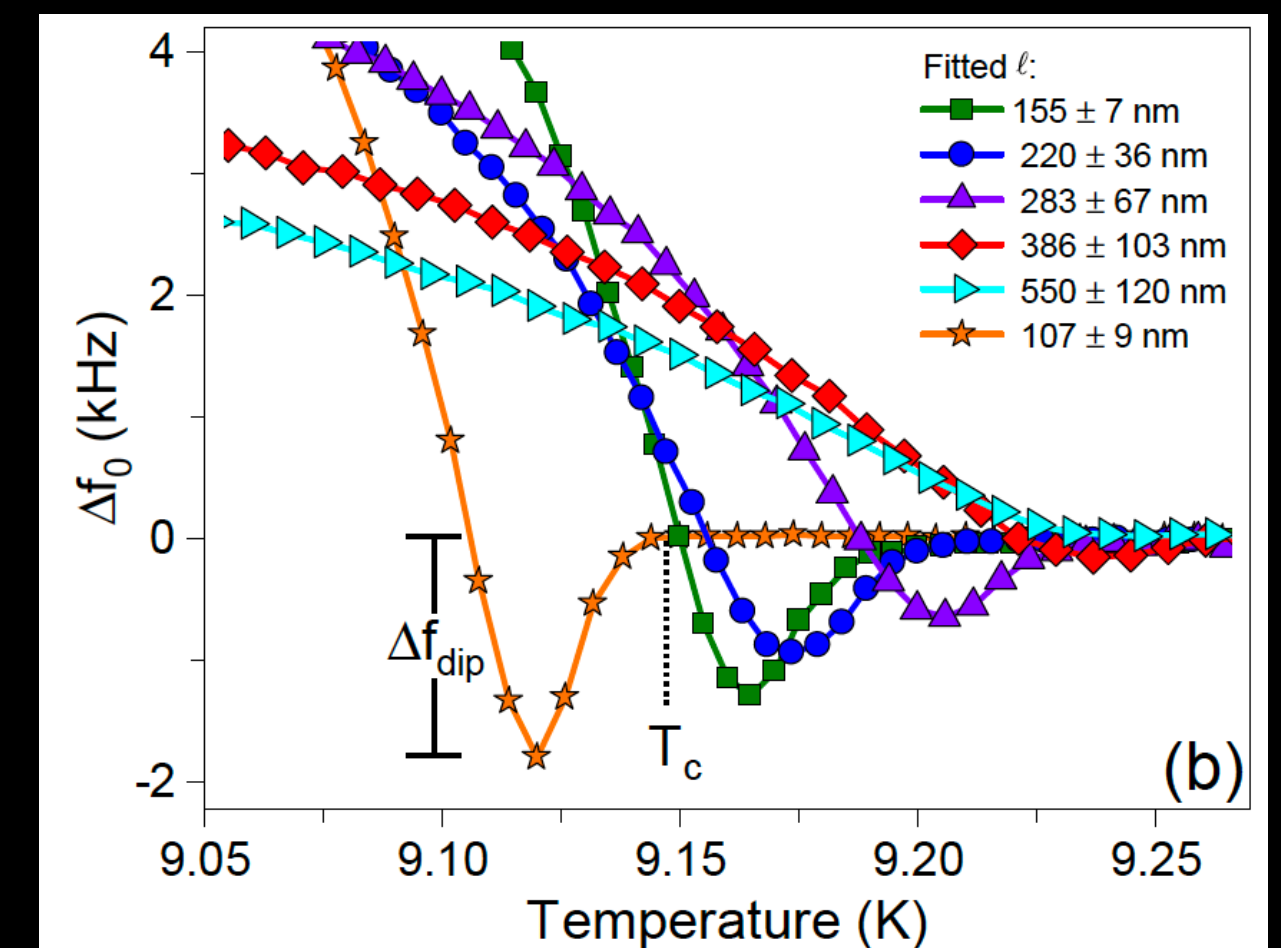


	Γ [ω]	Γ_s [ω]	Regime	ℓ [nm]	X_n [mΩ]	\tilde{f} [kHz]
Foot	0.33	26	$\Gamma \approx \omega \ll \Gamma_s \ll \Delta_0$	697	2.1	4.9
Bump	1.05	26	$\Gamma \approx \omega \ll \Gamma_s \ll \Delta_0$	679	2.1	5
D&B	1.5	26	$\omega \approx \Gamma \ll \Gamma_s \ll \Delta_0$	668	2.1	5.1
Dip A	5	26	$\omega \approx \Gamma < \Gamma_s \ll \Delta_0$	592	2.2	5.4
Dip B	5	50	$\omega \approx \Gamma \ll \Gamma_s \lesssim \Delta_0$	334	3	7.1
Dip C	5	100	$\omega \approx \Gamma \ll \Gamma_s \lesssim \Delta_0$	175	4.1	9.9
Dip D	0.33	100	$\Gamma \approx \omega \ll \Gamma_s \lesssim \Delta_0$	183	4	9.7

- Various regimes, under assumption of the local limit.



- Higher values of scattering rates reduce mean free path, reduce the T_c and deepen the dip.

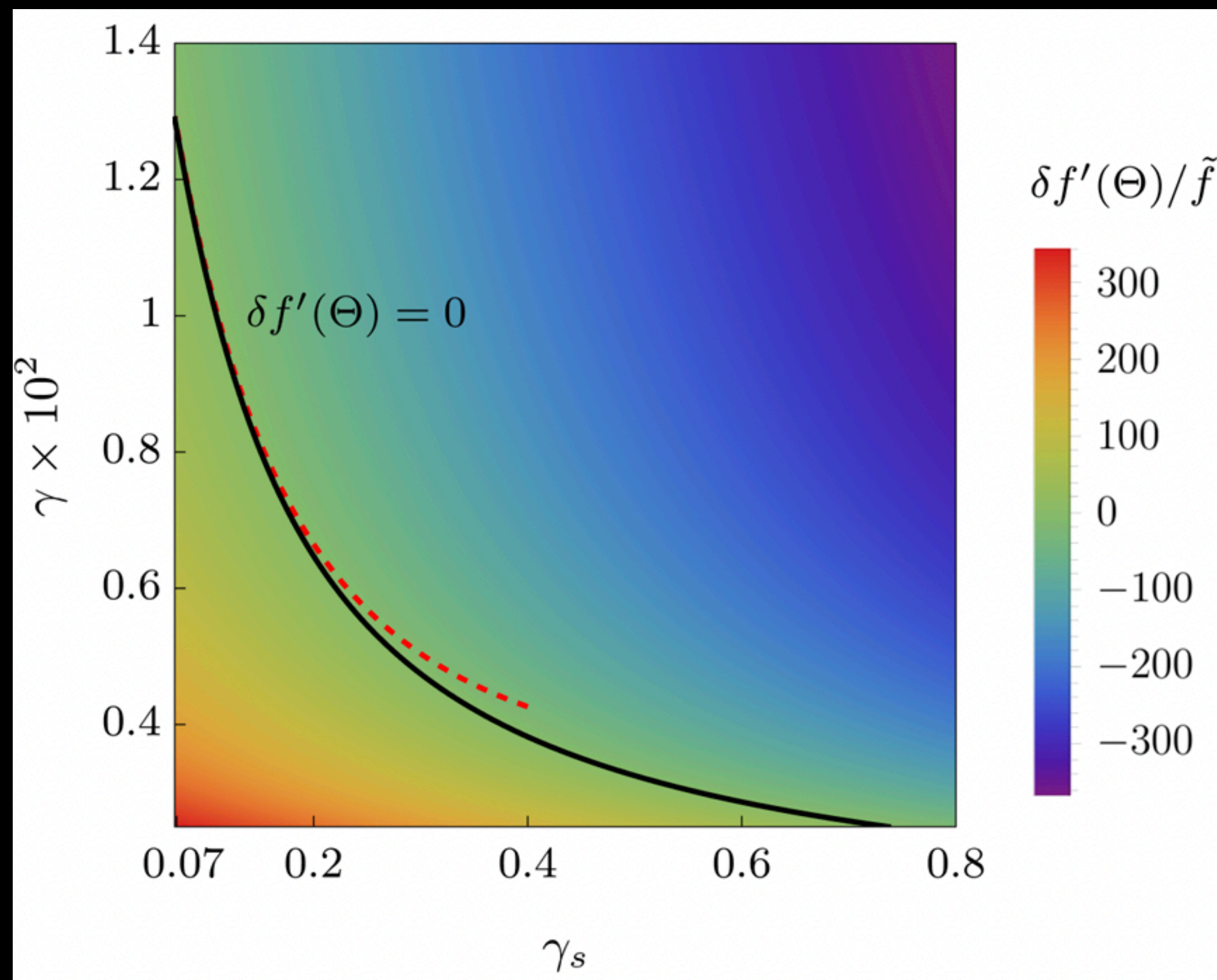


Moderately clean regime: $\hbar\omega < \Gamma \ll \Gamma_s \lesssim \Delta_0$

$$\delta f'(\Theta) \equiv \left. \frac{\partial \delta f(\Theta)}{\partial \Theta} \right|_{\Theta=0} \quad \text{where: } \Theta = 1 - T/T_c$$

$$\sigma'_s(T)/\sigma_0 = 1 + f_1(\Gamma, \Gamma_s)\Theta, \quad \sigma''_s(T)/\sigma_0 = f_2(\Gamma, \Gamma_s, \omega)\Theta.$$

$$\delta f(T \rightarrow T_c)/\tilde{f} = (f_1 - f_2)\Theta/2$$



1) $\Gamma \ll T_c \sim \Delta_{00}$

$$f_1(\Gamma, \Gamma_s) = \frac{\gamma_e \pi^2}{7\zeta(3)} \frac{\Gamma_s}{\Gamma_n} \frac{\Delta_{00}}{\Gamma}$$

$$f_2(\Gamma, \Gamma_s, \omega) = \frac{2\Gamma_n}{\omega} \frac{n_s(0)}{n} A$$

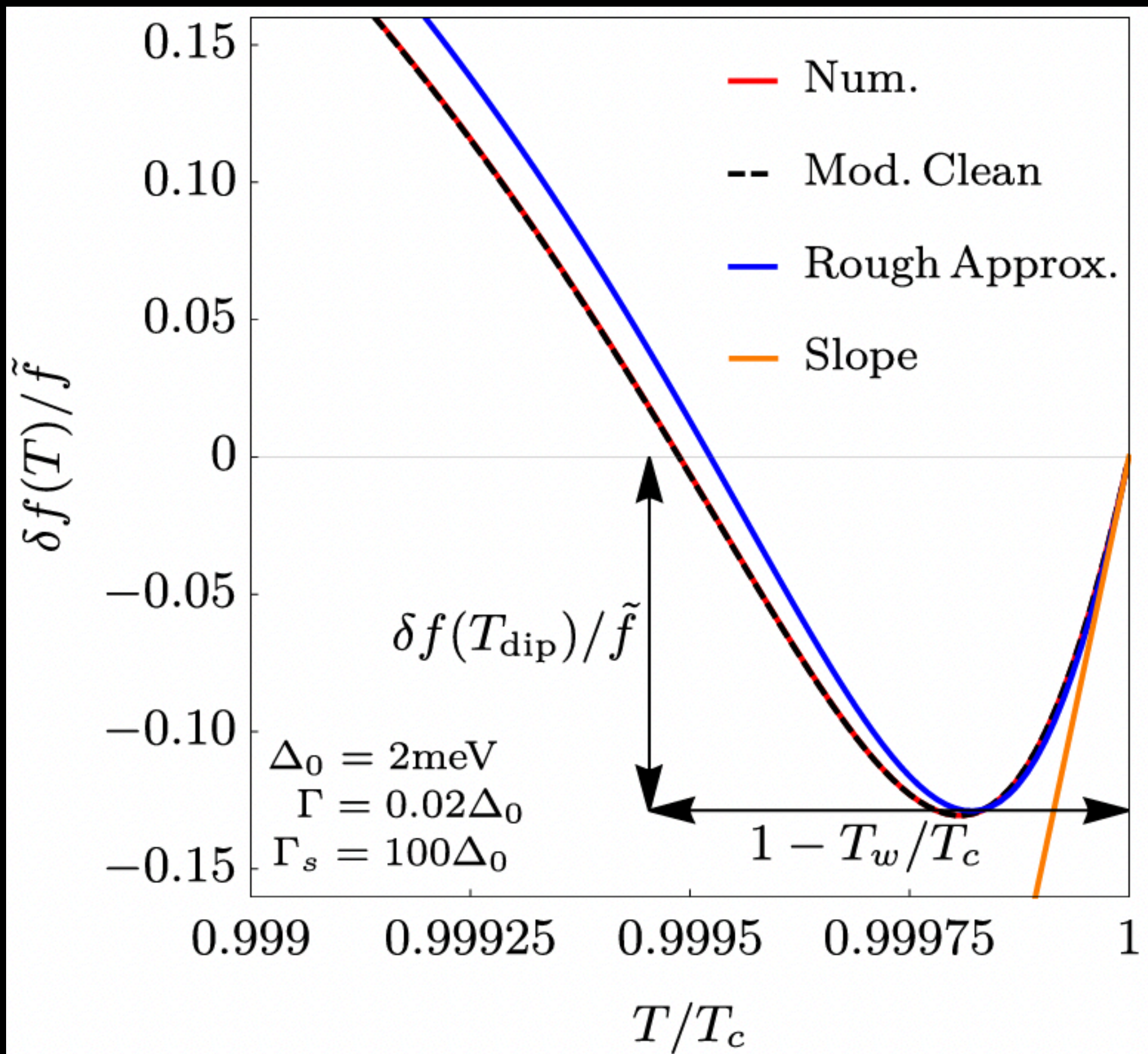
- Both signs are possible.

2) $\Gamma \gg T_c$ with arbitrary Γ_s

$$f_1 = -\frac{2\gamma_s + 3\gamma}{\gamma_s + \gamma} \frac{1}{\gamma^2} < 0$$

- Pure dip.

Dirty ideal limit: $\omega \ll \Gamma \ll \Delta(0) \approx \Delta_{00} \ll \Gamma_s$



Slope at T_{c0} :

$$\frac{\delta f(T)}{\tilde{f}} \approx \frac{2\gamma_e \pi^2}{7\zeta(3)} \frac{\Delta_{00}}{\omega} \left(\frac{\omega}{4\Gamma} - 1 \right) \left(1 - \frac{T}{T_{c0}} \right)$$

≈ 4.18

Width of the dip:

$$\delta f(T_w) = 0 \quad \text{for} \quad T_w \neq T_{c0}$$

$$\frac{T_w}{T_{c0}} \approx 1 - \frac{7\zeta(3)}{4\gamma_e \pi^2} \frac{\omega}{\Delta_{00}} \left(\sqrt{3} - \frac{\omega}{4\Gamma} \right)$$

Depth of the dip:

$$T_{dip} \approx T_w/3$$

$$\frac{\delta f(T_{dip})}{\tilde{f}} \approx -0.1398 + 0.082 \frac{\omega}{\Gamma}$$

Comparison & fitting the experimental dip

- No free parameters in comparison scenario.
- Pair-breaking fixed by the reduced T_c .

- Frequency scaling

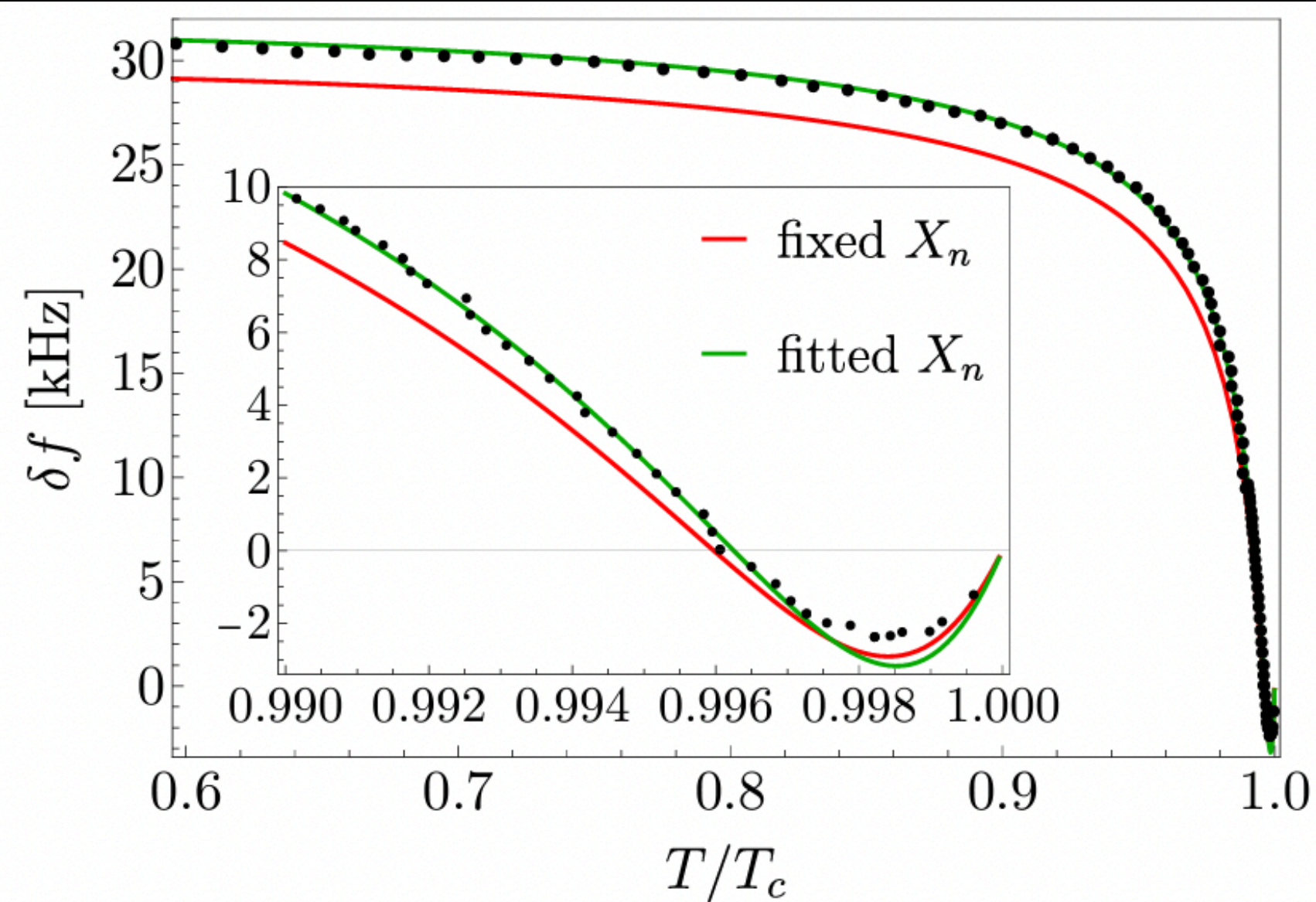


FIG. 7. Considered parameters: resonant frequency $f = 2.6$ GHz, $\Delta_0 = 1.55$ meV [1], pair-conserving scattering rate corresponding to fixed $X_n = 7.1$ m Ω (fitted $X_n = 7.5$ m Ω) is $\gamma_s = 0.52$ ($\gamma_s = 0.58$), and resulting $\ell = 121$ nm ($\ell = 108$ nm).

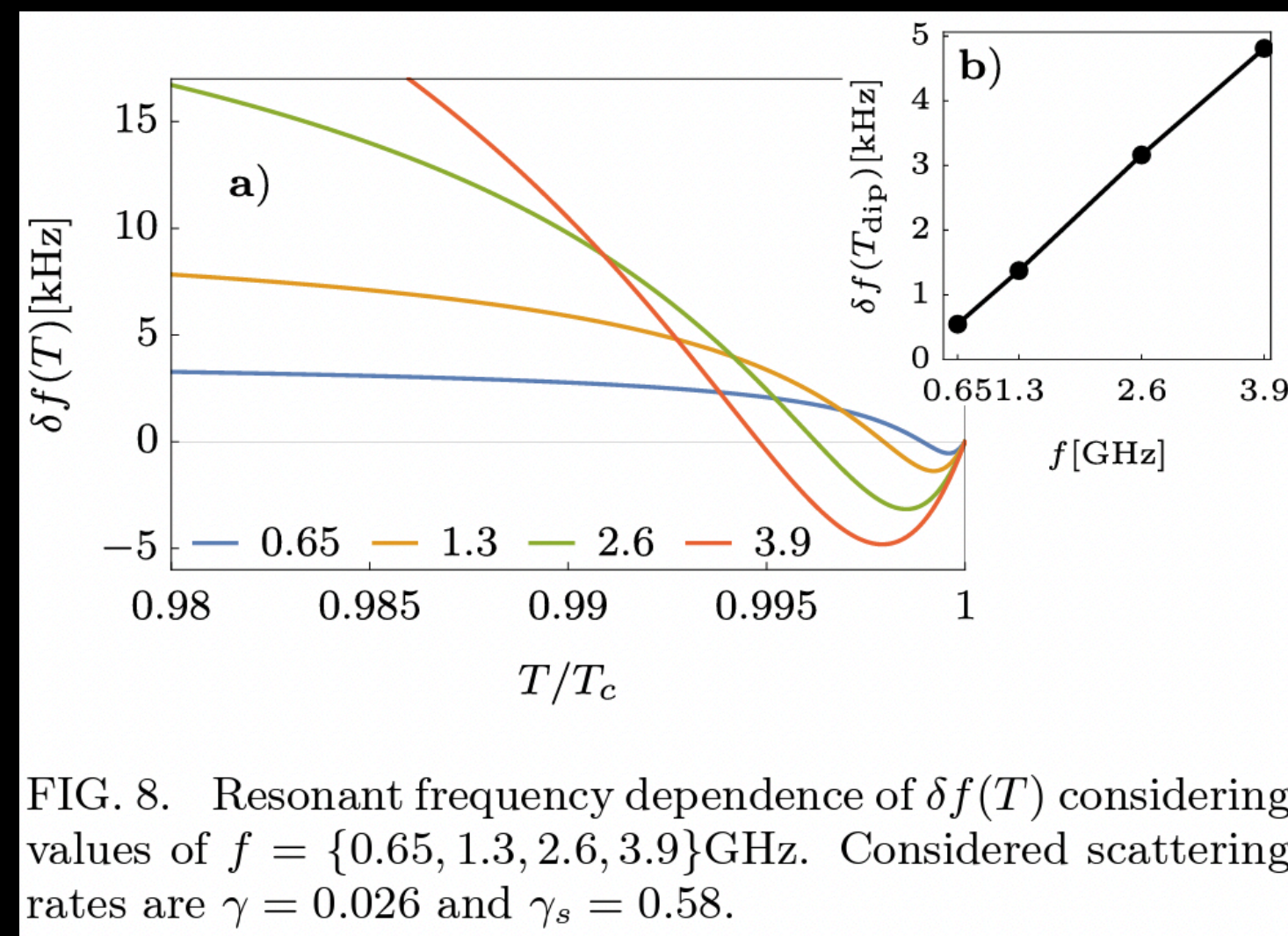
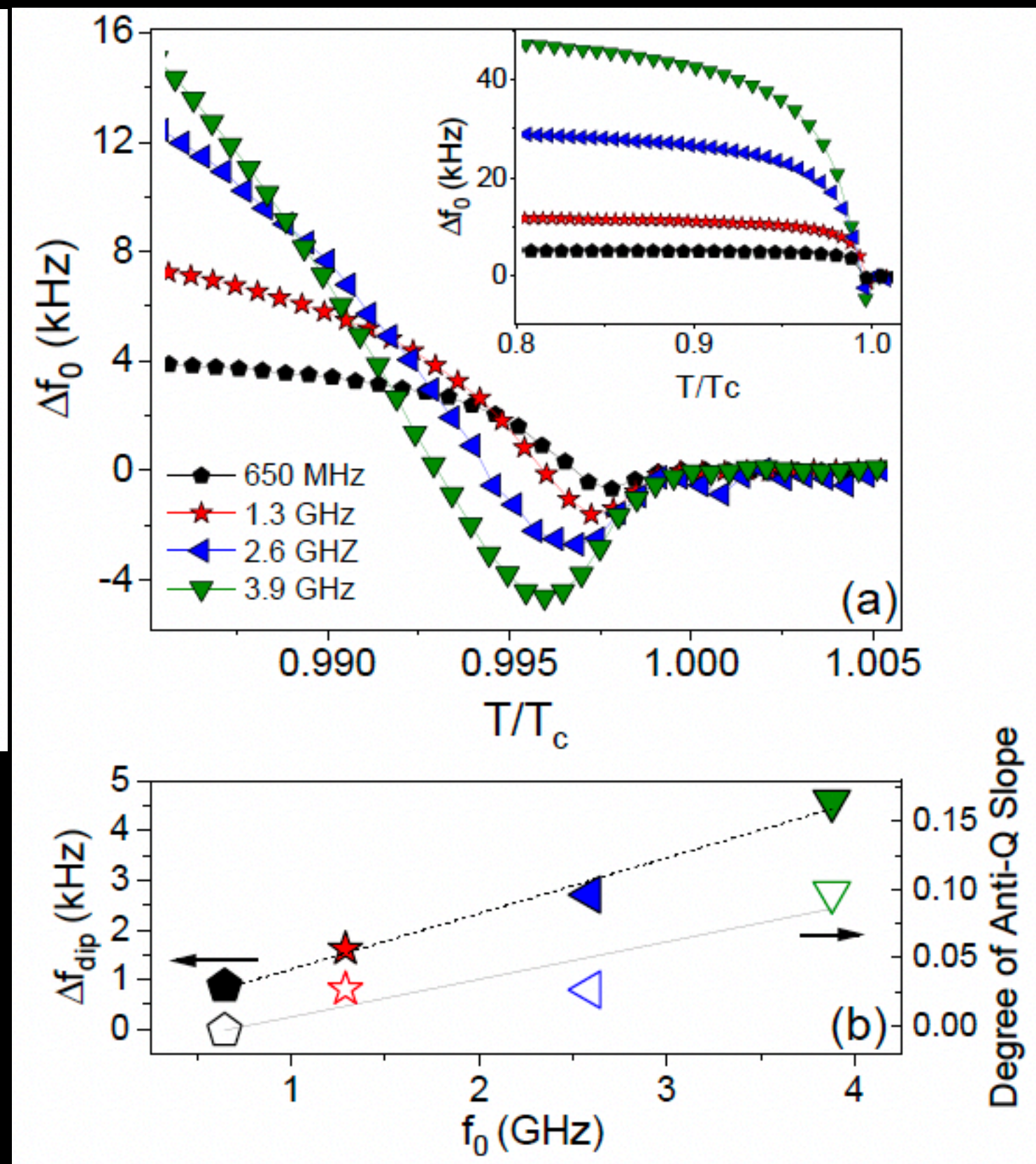


FIG. 8. Resonant frequency dependence of $\delta f(T)$ considering values of $f = \{0.65, 1.3, 2.6, 3.9\}$ GHz. Considered scattering rates are $\gamma = 0.026$ and $\gamma_s = 0.58$.



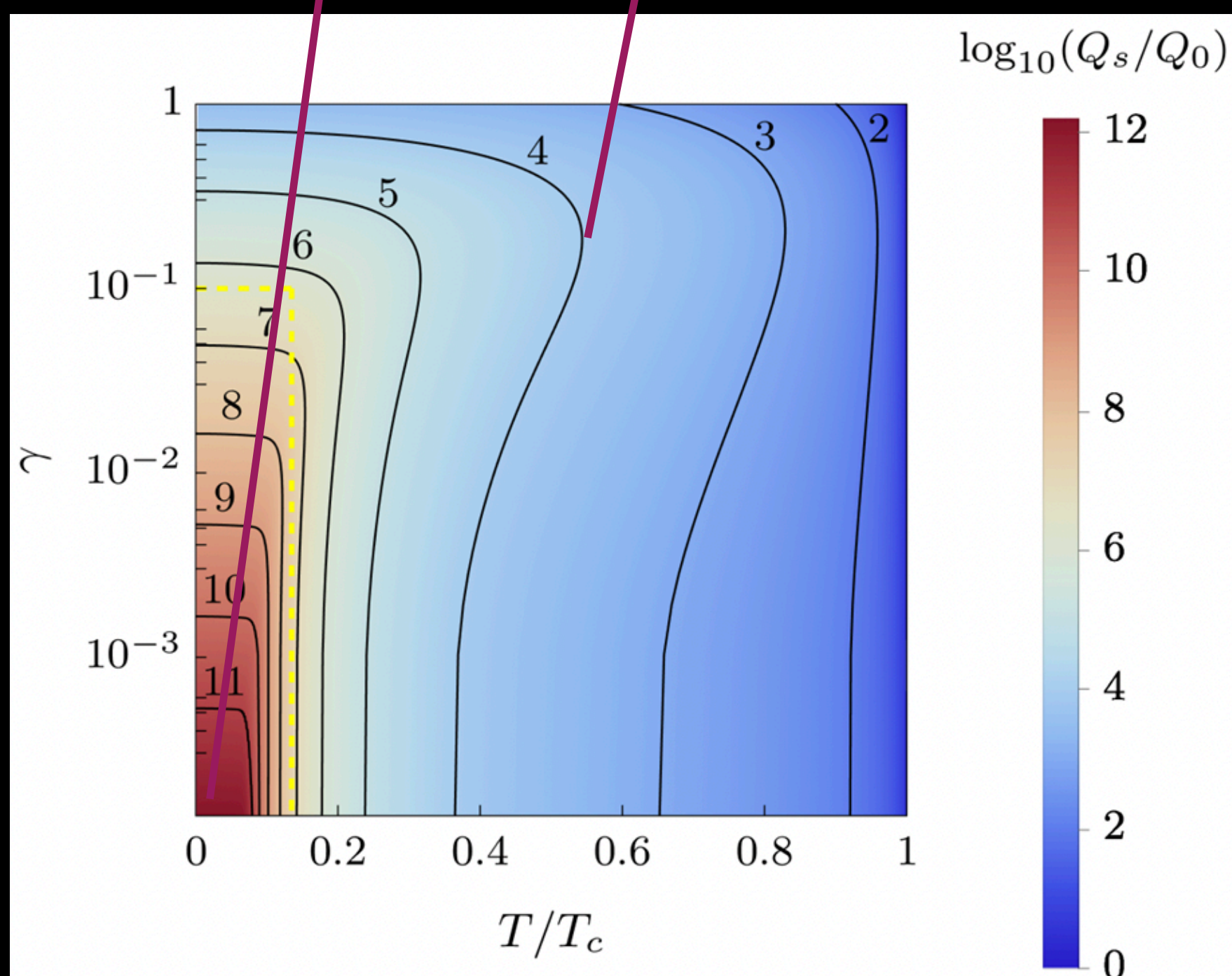
Quality $Q_s = G/R_s$ in local limit

$$\frac{Q_s}{Q_n} = \left(\frac{|\sigma_s|}{|\sigma_n|} \right)^{1/2} \frac{\cos(\pi/4)}{\cos(\pi/4 + \delta\varphi/2)}$$

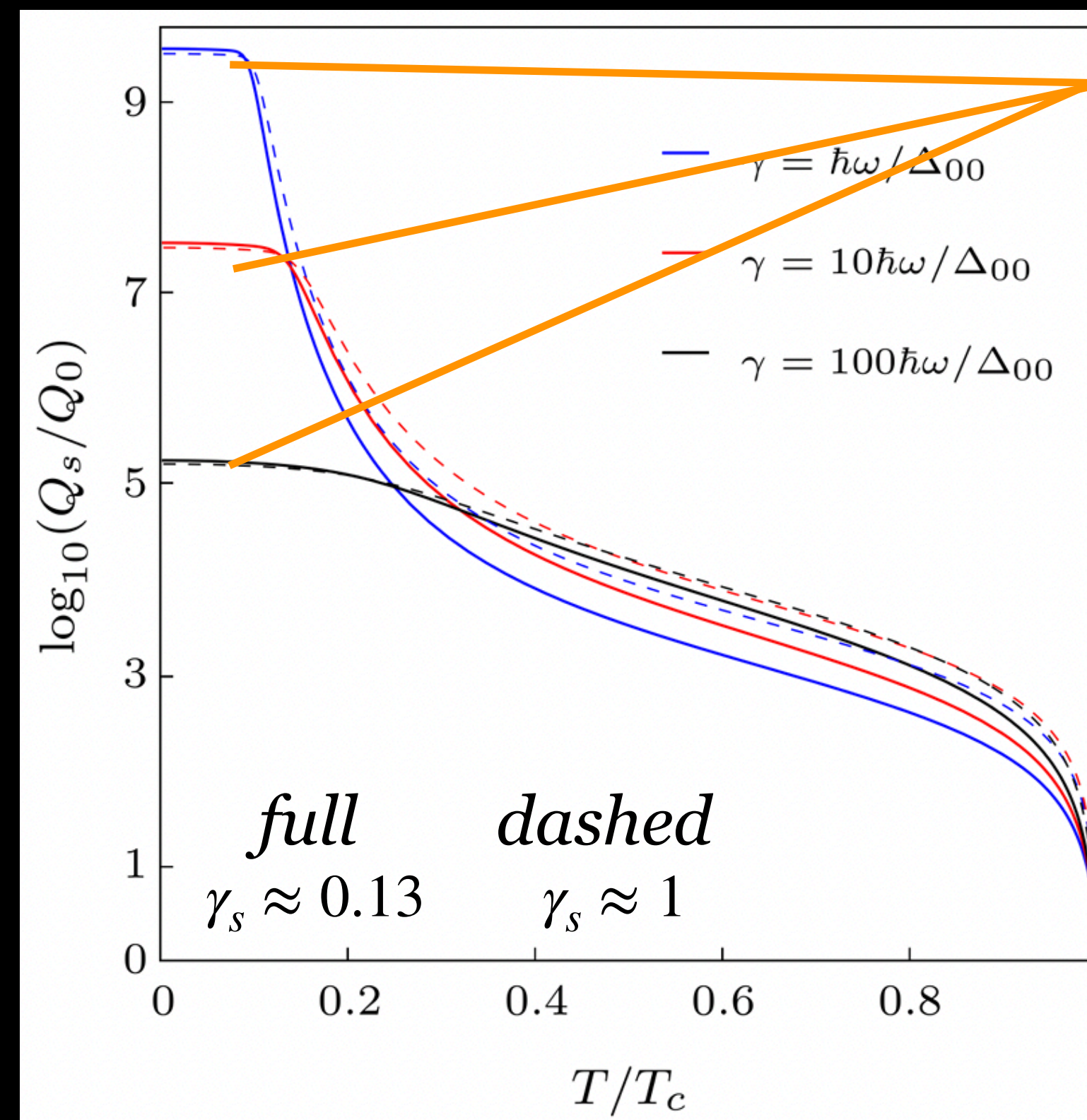
- Huge increase at low temperature due to low σ'_s and relatively high σ''_s .

• Absolute maxima at $T = 0K$, and $\gamma = 0$.

• Maximum for fixed $T \neq 0K$ at nonzero pair breaking.



$\gamma_s \approx 0.13$, $f = 1.3 \text{ GHz}$, $\Delta_{00} = 2 \text{ meV}$



• High Quality “plateaus” for $T \lesssim T_p \approx 0.1T_{c,0}$.

• Analysis showing the role of the in-gap states and Fermi-Dirac distribution can be found in [arXiv:2409.04203](https://arxiv.org/abs/2409.04203)

• Weakly dependent on $\gamma_s \lesssim 1$.

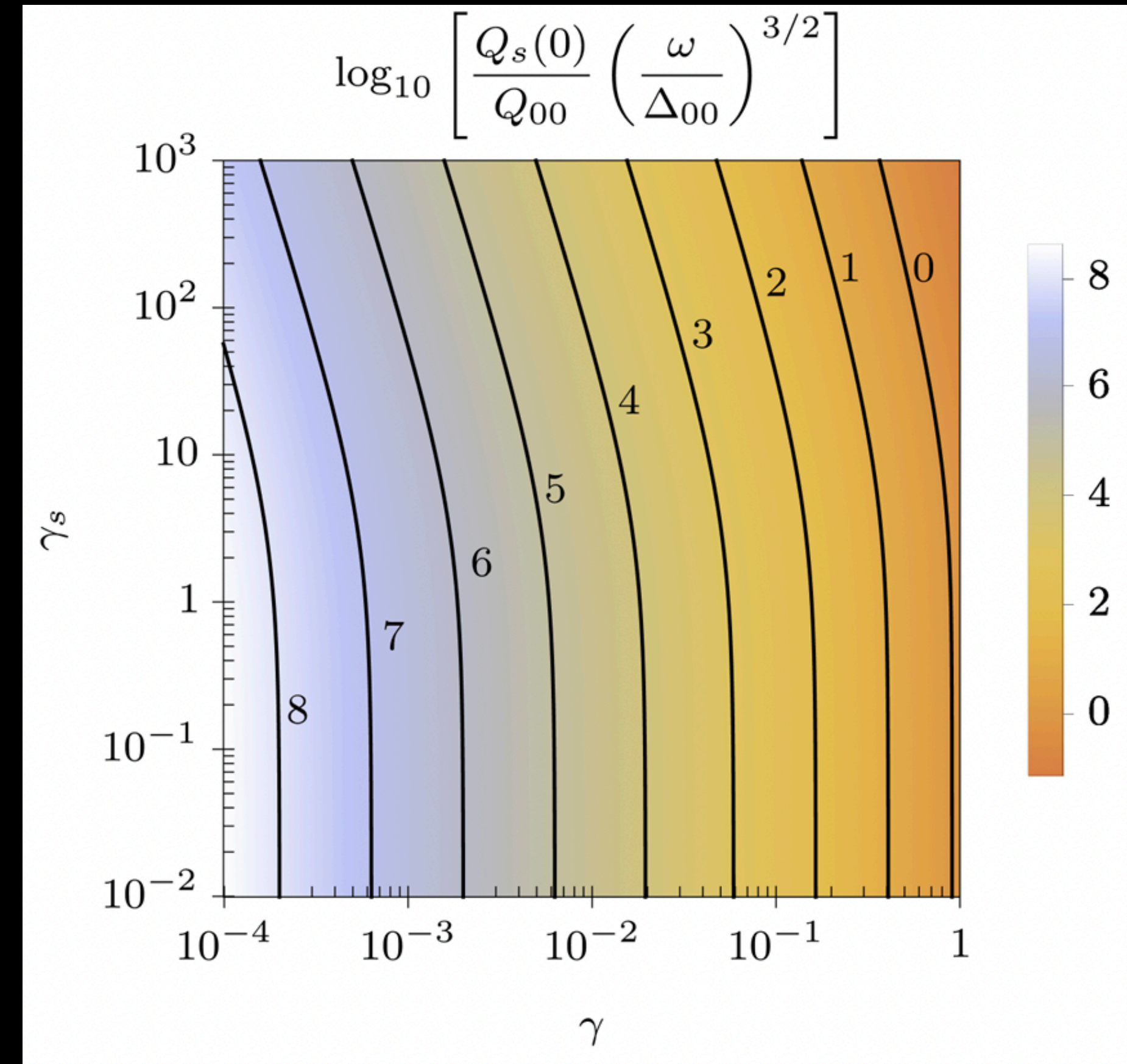
Quality at $T = 0K$

$$\frac{Q_s(0)}{Q_n} = \sqrt{\frac{2}{\sigma_0} \frac{\sigma_s''(0)^{3/2}}{\sigma_s'(0)}} = \frac{4\sigma_0}{\sigma_s'(0)} \left(\frac{n_s(0)}{n} \frac{\Gamma + \Gamma_s}{\omega} \right)^{3/2}$$

- Role of superfluid fraction.

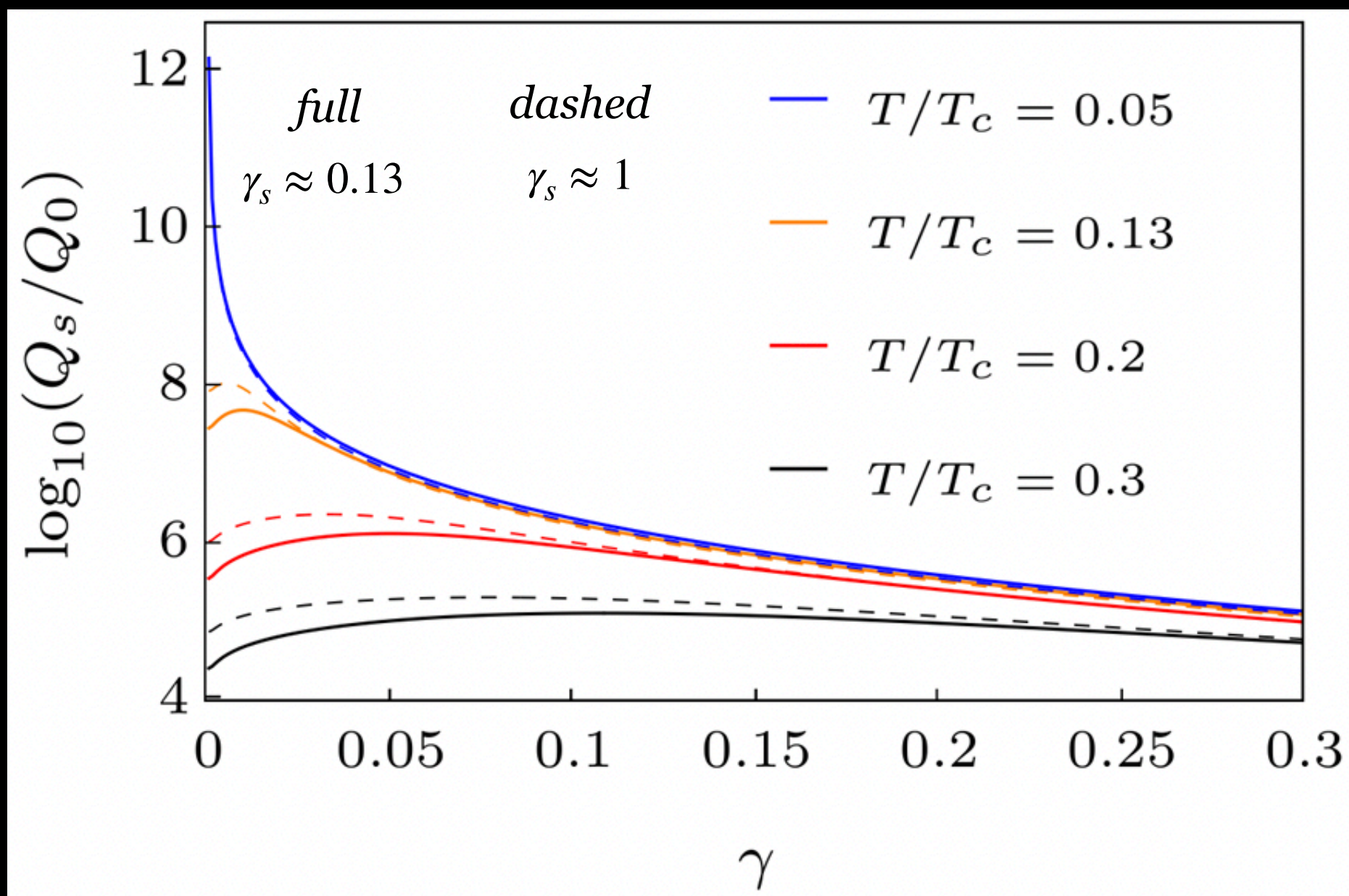
$$\frac{\sigma'(0)}{\sigma_0} = \frac{\gamma^2}{1 + \gamma^2} \times \frac{\gamma_s + \gamma}{\gamma_s + \sqrt{1 + \gamma^2}}$$

- Pair-breaking subgap induced residual resistance.



- The different roles of pair-breaking and pair-conserving scattering.

- Role of pair-conserving disorder changes.



Superfluid fraction

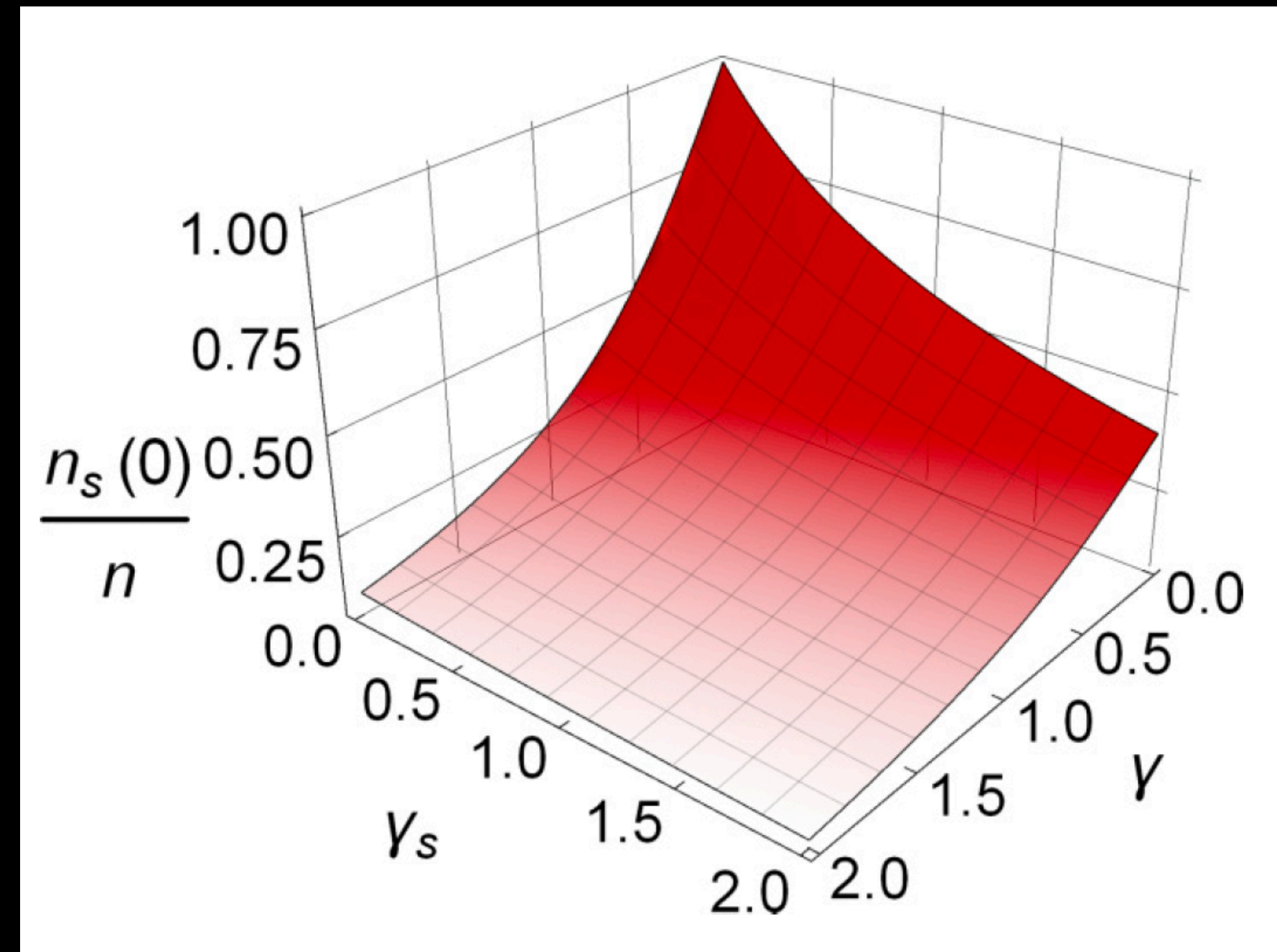
$$n_s(0)/n = \begin{cases} \frac{1}{\gamma_s} \left[\arctan(1/\gamma) - \frac{1}{\sqrt{1-\gamma_s^2}} \left(\arccos \gamma_s + \arctan \frac{\sqrt{1-\gamma_s^2}}{\gamma} - \arctan \frac{\sqrt{1-\gamma_s^2} \sqrt{1+\gamma^2}}{\gamma \gamma_s} \right) \right], & \text{if } \gamma_s < 1 \\ \frac{1}{\gamma_s} \left[\arctan(1/\gamma) - \frac{1}{\sqrt{\gamma_s^2-1}} \ln \frac{(\gamma_s + \sqrt{\gamma_s^2-1})(\gamma + \sqrt{\gamma_s^2-1})}{\gamma \gamma_s + \sqrt{\gamma_s^2-1} \sqrt{\gamma^2+1}} \right], & \text{if } \gamma_s \geq 1 \end{cases}$$

- Assuming $\gamma_s < 1$ and linear order of γ :

$$\frac{n_s(0)}{n} = \frac{1}{\gamma_s} \left[\frac{\pi}{2} - \frac{\arccos \gamma_s}{\sqrt{1-\gamma_s^2}} \right] - \frac{\gamma}{\gamma_s + 1}$$

- Assuming $\gamma_s \ll 1$ and $\gamma \ll 1$:

$$n_s(0)/n \approx 1 - \gamma - \gamma_s \pi/4$$

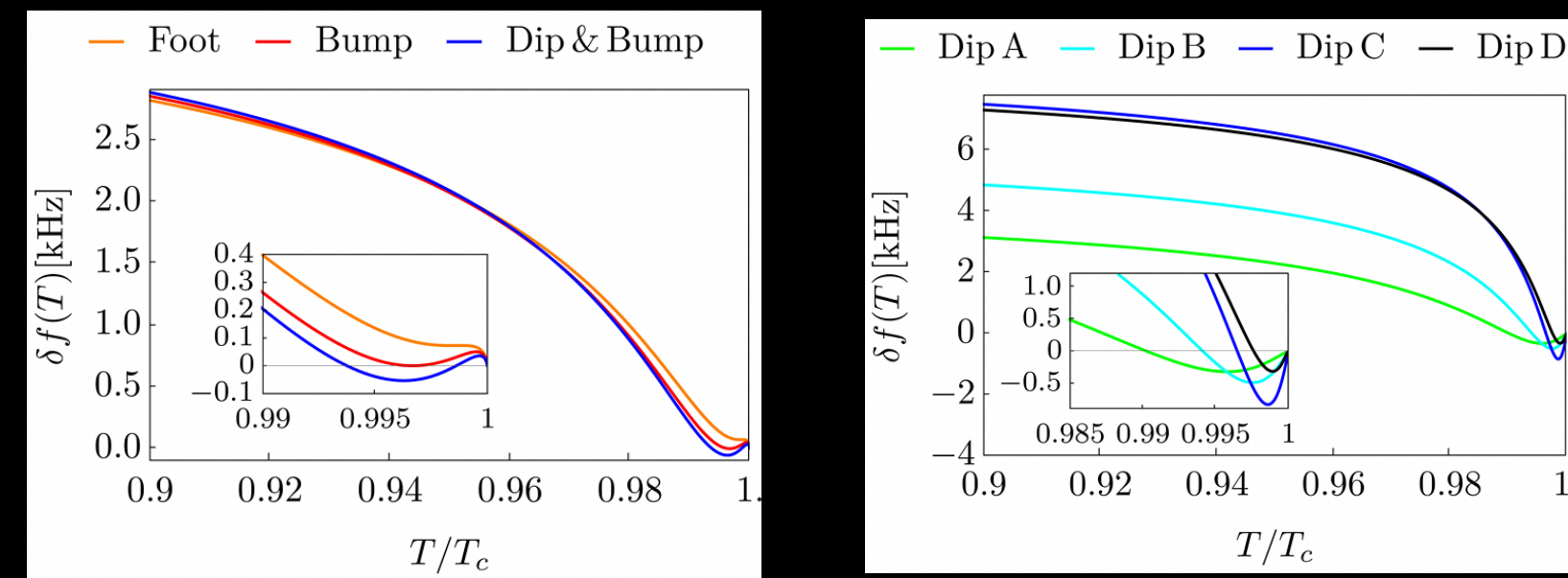


Summary & Conclusions I.

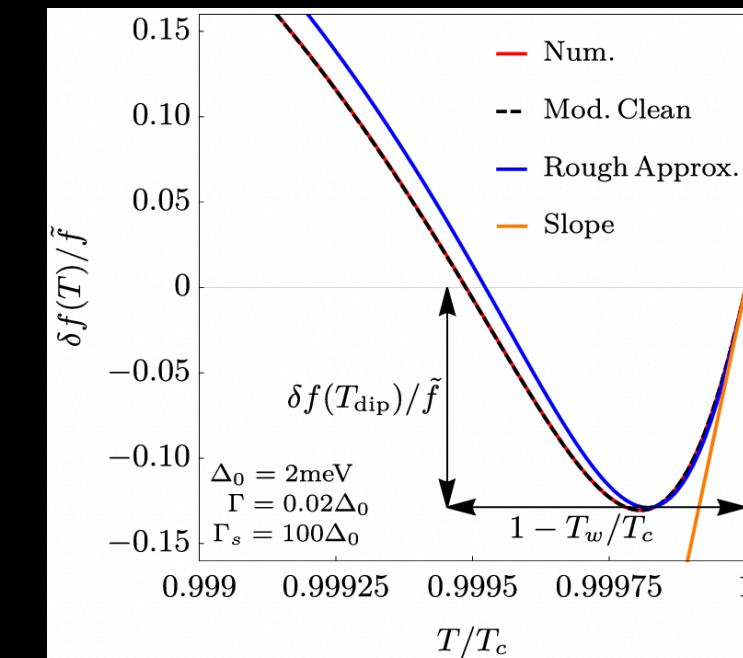
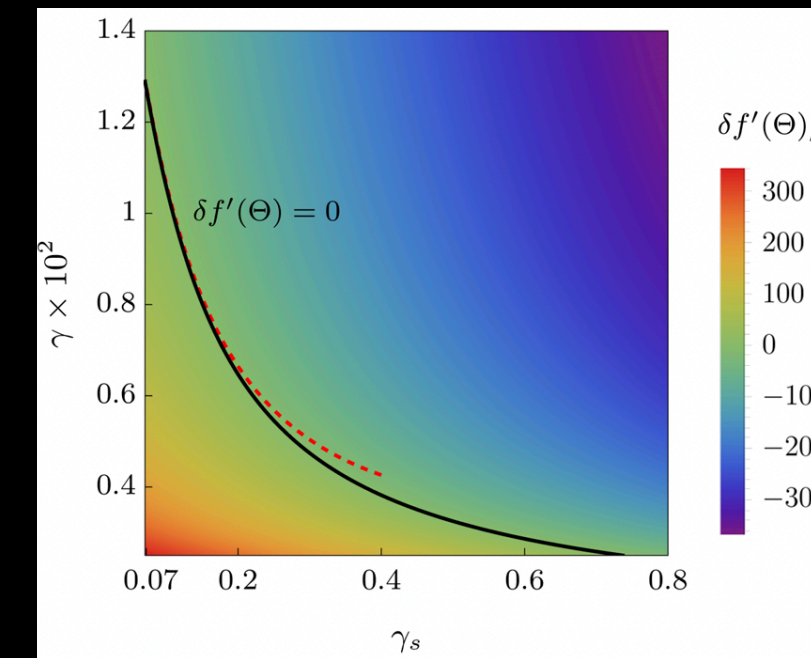
Frequency Shift

- Despite omitting the inhomogeneity effects, DS framework provides qualitatively (and quantitatively) reasonable results with the same numerical complexity as the Mattis-Bardeen theory.

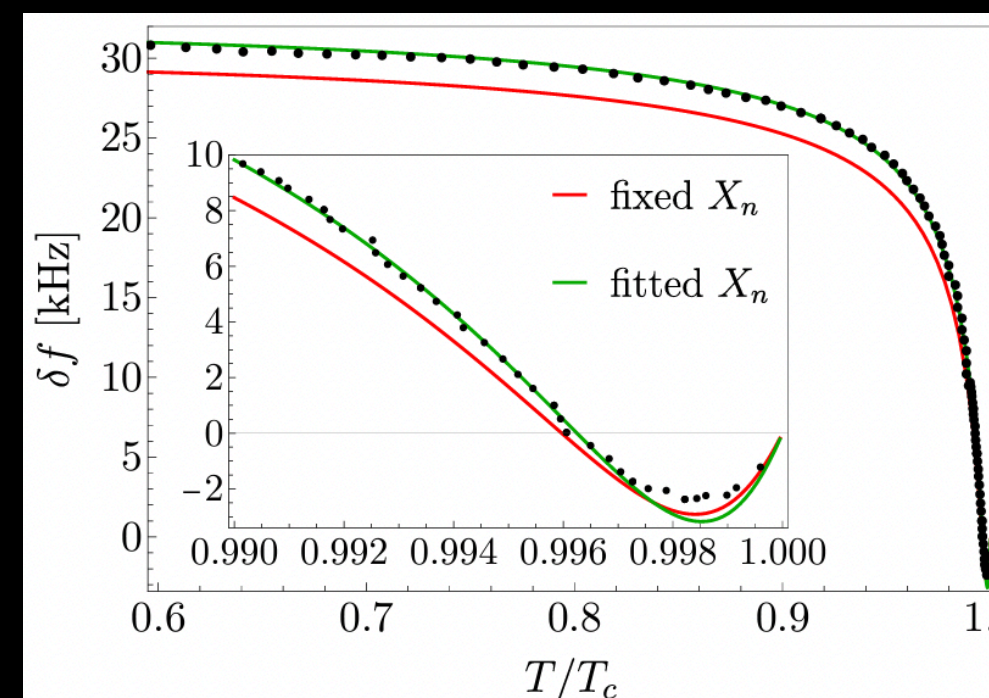
- Various frequency shift regimes (Foot, Bump, Dip & Bump and Dip) assuming low disorder can be systemically identified.



- Addressing the moderately clean regime, we describe the frequency shift slope $\delta f'(\Theta) = \partial \delta f(\Theta) / \partial \Theta |_{\Theta=0}$ with the simple function of pair-conserving and pair-breaking scattering rates.



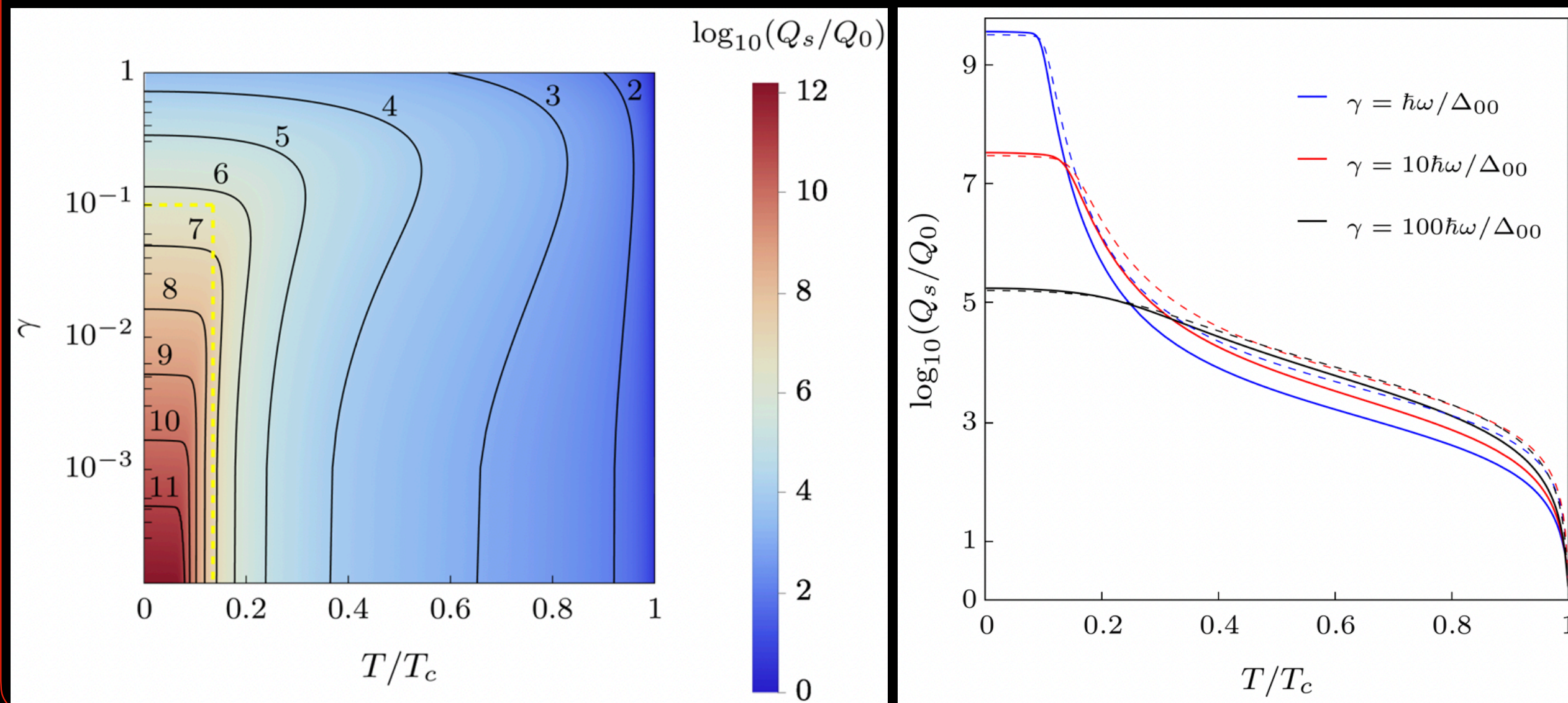
- Considering the complexity of the phenomena together with the relevant temperature scale and simplicity of our approach, we achieve compelling agreement with the experiment.



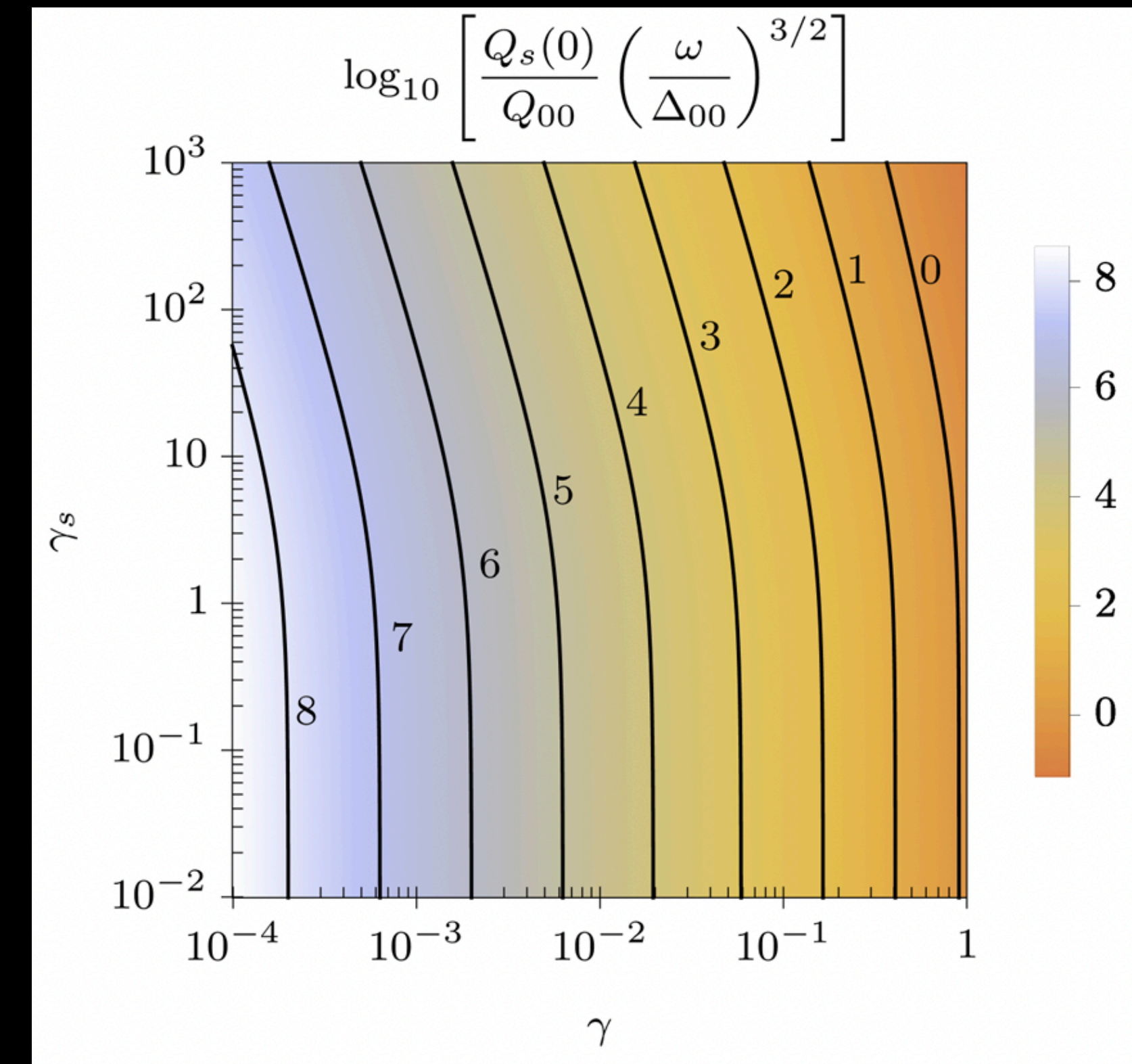
Summary & Conclusions II.

Quality

- Analysis of the high quality plateaus at low temperature and low disorder. For details see: [arXiv:2409.04203](https://arxiv.org/abs/2409.04203).



- Analysis of the quality factor at zero Kelvin Temperature shows different influence of pair-breaking and pair-conserving disorder.



Publications Related to the Dynes superconductivity

- F. Herman and R. Hlubina, Phys. Rev. B **108**, 134518 (2023),
Slope of H_{c2} close to T_c versus the size of the Cooper pairs: The role of disorder in Dynes superconductors,
- F. Herman, Phys. Rev. B **106**, 224521 (2022),
Advanced approach of superconducting gap function extraction from tunneling experiments,
- D. Kavický, F. Herman and R. Hlubina, Phys. Rev. B **105**, 214504 (2022),
Model-independent determination of the gap function of nearly localized superconductors,
- F. Herman and R. Hlubina, Phys. Rev. B **104**, 094519 (2021),
Microwave response of superconductors that obey local electrodynamics,
- F. Herman and R. Hlubina, Phys. Rev. B **97**, 014517 (2018),
Thermodynamic properties of the DS,
- F. Herman and R. Hlubina, Phys. Rev. B **96**, 014509 (2017),
Electromagnetic properties of impure superconductors with pair-breaking processes,
- F. Herman and R. Hlubina, Phys. Rev. B **95**, 094514 (2017),
Consistent two-lifetime model for spectral functions of superconductors,
- F. Herman and R. Hlubina, Phys. Rev. B **94**, 144508 (2016),
Microscopic interpretation of the Dynes formula for the tunnelling density of states

Open question

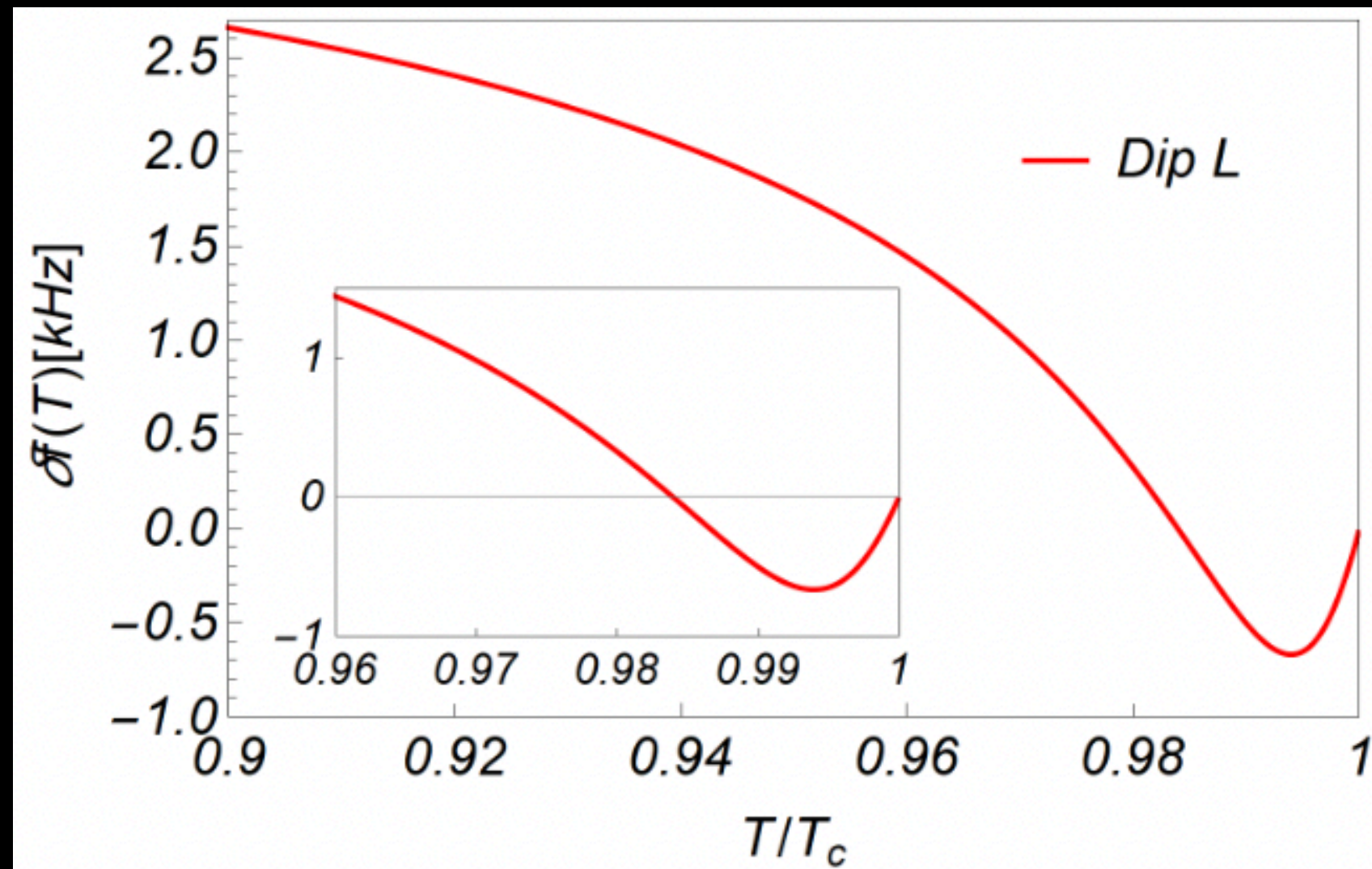
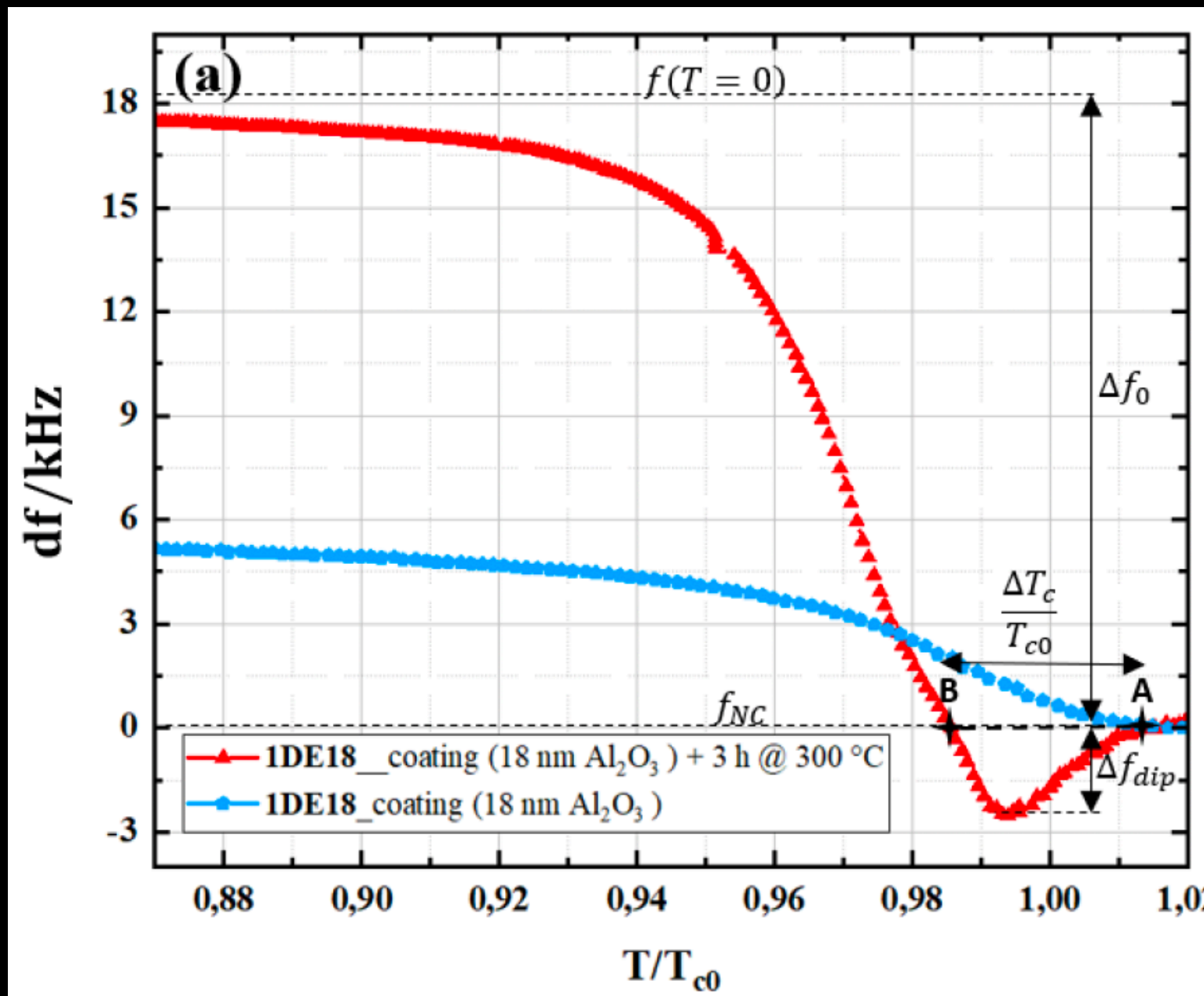


FIG. 1. Dip on the scale of $\sim 0.01T_c$.



	$\Gamma[\omega]$	$\Gamma_s[\omega]$	Regime	$\ell[\text{nm}]$	$X_n[\text{m}\Omega]$	$\tilde{f}[\text{kHz}]$
Dip L	26	0.01	$\Gamma_s \ll \omega \ll \Gamma \lesssim \Delta_0$	706	2	4.9

TABLE I. Table of individual regimes together with its considered scattering constants Γ and Γ_s in units of the angular resonant frequency $\hbar\omega$ (for convenience $\hbar = 1$, and $f = 1.3$ GHz). For each regime, we also add the parameter inequalities as well as calculated values of mean free path ℓ , normal state reactance X_n , and the scale \tilde{f} .

Role of the 18 nm layer of Al_2O_3 , or oxides in general?

Mean free path ℓ ?

Comparison of Approaches